

Contents lists available at ScienceDirect

Physica D

journal homepage: www.elsevier.com/locate/physd





Phase boundary dynamics for ice nucleation and growth processes in fresh and sea water

Bernd Kutschan a,*, Silke Thoms a, Andrea Thom b, Raghav Pathak b, Tim Ricken b

- ^a Alfred Wegener Institute Helmholtz Centre for Polar and Marine Research, Ecological Chemistry, Am Handelshafen 12, 27 570 Bremerhaven, Germany
- b University of Stuttgart, Institute of Structural Mechanics and Dynamics in Aerospace Engineering and Geodesy, Pfaffenwaldring 27, 70 569 Stuttgart, Germany

ARTICLE INFO

Communicated by Jesus Cuevas-Maraver

Keywords: Sea ice Crystal growth Phase transition

ABSTRACT

Ice crystals and snowflakes are out-of-equilibrium growth shapes which are a result of a nonlinear growth dynamics as a consequence of the extremal property of the associated thermodynamic potential. A special role during the pattern formation play kink solutions that represent the different state of order at the phase boundaries. The mechanisms of the kink formation give an insight into the dynamics of phase transitions in particular the formation and growth of ice nuclei. In this paper is described a relationship between the classical nucleation theory and Kobayashi's phase field theory for ice crystal growth. The critical length of the nuclei is derived from the linear stability analysis for the phase field model and is identified with the result of the classical nucleation theory. We modify original Kobayashi's phase field model by including freezing point depression due to salt in order to describe the phase boundary of the fine network and cavities filled with brine which are formed during the freezing process in sea ice.

1. Introduction

In atmosphere as well as on supercooled surfaces or in polar regions of the ocean, structures form spontaneously in supercooled water. An unmanageable number of water models shows the incompleteness of our understanding of water [1]. Sodium and chloride ions are another challenge in freezing salt solutions [2], although seawater also contains many other halides and ions [3] with CaCO₃ precipitation in sea ice and presence of ikaite [4]. In addition, diverse organic substrates can act as ubiquitous biological ice nucleators both in clouds [5,6]. The kind of the growth of ice crystals should allow us to draw conclusions from the environmental conditions in the atmosphere or in water-ice interface if the mechanisms of the anisotropic growth are known. Nakaya used to say, the morphology of snow crystals are like hieroglyphs sent to us from the sky [7].

First, each complex phenomenon should break down into its essential processes and we use phase field methods on mesoscopic scale. This approach can describe very different appearances of crystals as fern-like dendrite pattern [8–11] and can also be found on the freezing soap bubble (see Fig. 1) or as hexagonal prisms (see Fig. 2). Other authors has been investigated the morphological instability of the Saffman–Taylor finger depending on the surface tension and the growth of side branches [12–14] or discuss the difference between a diffuse interface (Cahn–Hilliard models) [15–17] and a sharp interface (Stefan and Hele-Shaw problem [18–21] or the morphological instability according to

Sekerka [22]. In particular, the anisotropic Hele-Shaw flows is analyzed experimentally and theoretically in various papers [23-27] using complex analysis. On the other hand any curve in the plane may be parametrized by the arc length (natural representation) and measured by the differential-geometric invariant called the curvature. A corresponding differential-geometric evolution equation for the interface is studied in different publications [28-32]. A rigorous asymptotic analysis of Caginalp's model leads to the Gibbs-Thomson condition which relates the temperature at the interface to the surface tension and curvature. An alternative model to the Caginalp framework is derived by Penrose and Fife [33]. They published a thermodynamically consistent phase field type model for the kinetics of phase transitions. Due to the integrating factor referred to above, the Penrose-Fife model includes more mathematical difficulties than the Caginalp-approach. For this reason the Caginalp model is used mostly [34]. Kobayashi [35,36] simulated both hexagonal ice crystals and dendritic structures during the supercooling solidification without discontinuity in the first derivative of the free energy and Wheeler et al. analyzed the method concerning the realistic assumptions [37]. In Fig. 1(a) we generated a density plot of the order parameter $0 \le \eta(\zeta) \le 1$ using the Kobayashi model. The order parameter is also called the phase field. Gránásy [38] proposed a Cahn-Hilliard-type model of ice nucleation for a radially symmetric case. In this case, the three-dimensional problem can be reduced to a

E-mail address: bernd.kutschan@awi.de (B. Kutschan).

^{*} Corresponding author.

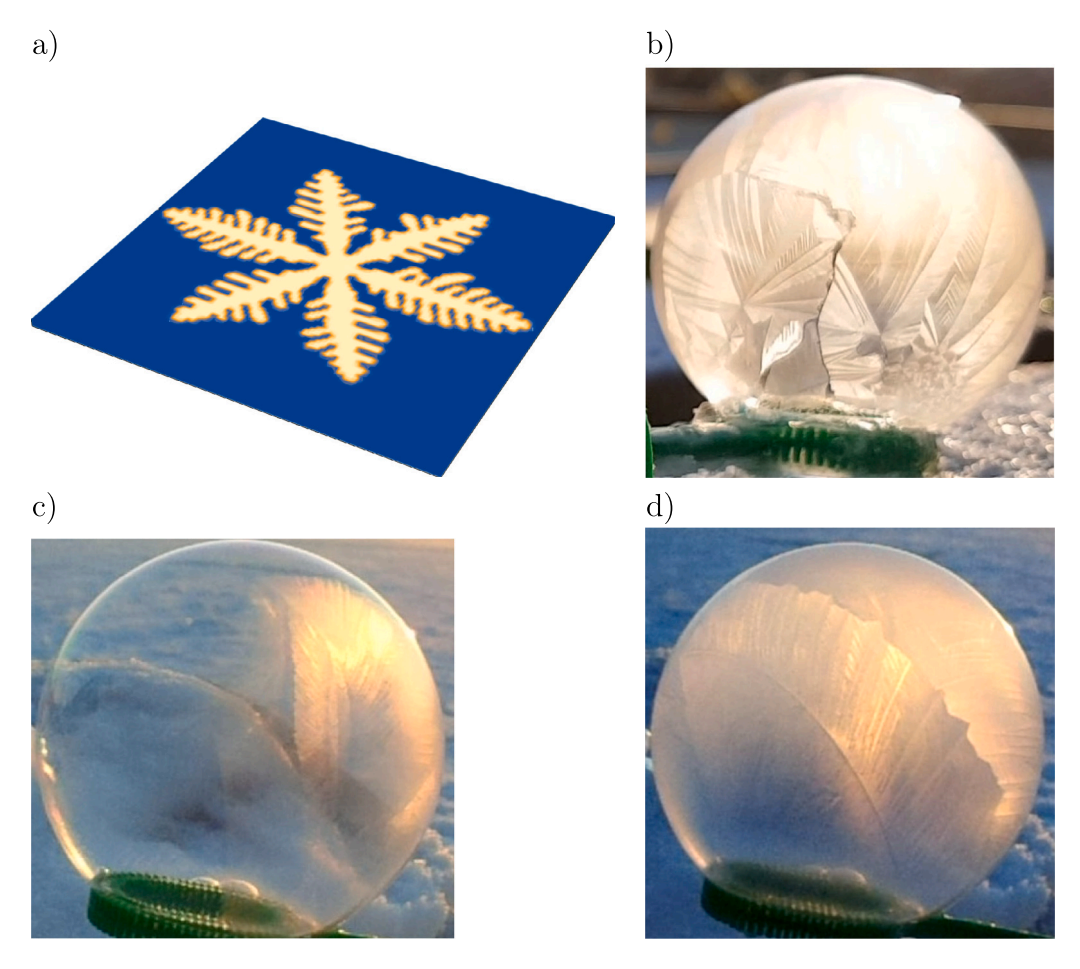


Fig. 1. Different appearance of crystals: (a) Two dimensional simulation correspond to the Kobayashi-model, (b) snapshot of a frozen soap bubble, December 2021, (c) & (d) two time steps of freezing soap bubble, February 2021 (private recordings).

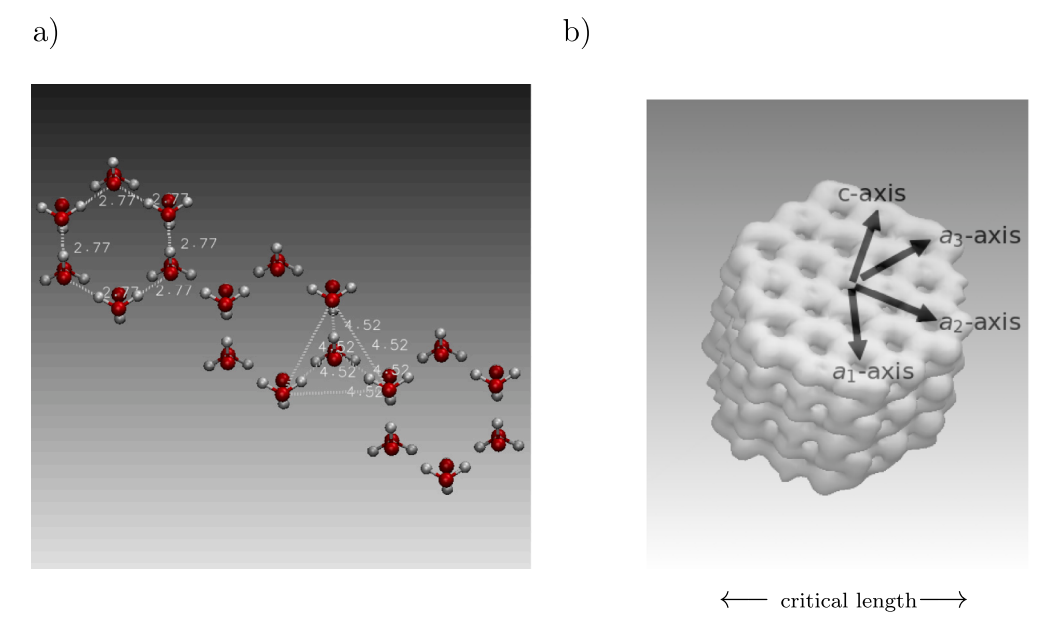


Fig. 2. (a) The oxygen atoms of ice forms a tetraeder with distances of 4.52 Å. (b) Critical length of a nucleus corresponds to about 5 hexagonal rings.

Table of symbols Dimensional quantities		
	-	Unit
Symbol	Name	
c	Experimental freezing velocity	$1\frac{m}{s}$
f_{LG}	Landau–Ginzburg free energy density	$1 \frac{J}{m^3} = 10 \frac{\text{erg}}{\text{cm}^3}$
F_{LG}	Landau-Ginzburg free energy	$1 J = 10^7 \text{ erg}$
ΔG	Gibbs free energy difference	$1 J = 10^7 \text{ erg}$
$\Delta G_{tot} \ \Delta G_c$	Gibbs free energy barrier	$1 J = 10^7 \text{ erg}$ $1 J = 10^7 \text{ erg}$
ΔG_c	Gibbs free energy barrier at critical radius (maximum)	$IJ = 10^{\circ} \text{ erg}$
Δg_v	Gibbs free energy density difference	$1 \frac{J}{m^3} = 10 \frac{erg}{cm^3}$
ΔH	Helmholtz free energy difference	$1 J = 10^7 erg$
k_B	Boltzmann constant	$1.38 \cdot 10^{-23} \frac{J}{K}$
K_F	Cryoscopic constant	$1\frac{\text{K kg}}{\text{mol}}$
h	Molecular spacing	$1 \text{ m} = 10^{10} \text{ Å}$
M	Molar mass	$1 \frac{\text{kg}}{\text{mol}} = 10^3 \frac{\text{g}}{\text{mod}}$
n	Amount of substance	1 mol
N_A	Avogadro constant	$6.02 \cdot 10^{23} \frac{1}{\text{mol}}$
q	Latent heat water (fusion)	$6.02 \cdot 10^{23} \frac{1}{\text{mol}} $ $3.33 \cdot 10^9 \frac{\text{erg}}{\text{g}}$
r	Radius of nucleus	1 m
r_c	Critical radius	1 m
r_a	Length at $\Delta G_{tot} = 0$	1 m
r_0	Scaling factor Salinity	1 m
ΔS	•	$1 \frac{g}{kg}$
Δ3 Τ	Entropy difference Applied temperature	$1 \frac{J}{K}$ 1 K
T_0	Melting point of pure water	1 K
T_s	Lowest supercooling temperature of pure water	1 K
ΔT	Temperature difference between applied temperature and lowest supercooling temperature	1 K
ΔT_0	Temperature difference between melting point and lowest	1 K
t	supercooling temperature Time	1 s
t_0	Time scaling factor	1 s
t_1	Time scaling factor	1 s
V	Nucleus volume	1 m ³
V_m	Molar volume of water	$18 \frac{\text{cm}^3}{\text{mol}}$
z	Length	1 m
z_0	Length scaling factor	1 m
z_1	Length scaling factor	1 m
γ_{sl}	Surface tension solid/liquid	1 erg cm ²
γ_{sv}	Surface tension solid/vapour	$1 \frac{\text{erg}}{\text{cm}^2}$ $1 \frac{\text{erg}}{\text{cm}^2}$
γ_{lv}	Surface tension liquid/vapour	1 cm ²
$\Delta \gamma$	Surface tension (remelting process)	$1 \frac{\text{erg}}{\text{cm}^2}$
γ	Surface tension (nucleation process)	$1 \frac{\text{erg}}{\text{cm}^2}$
$\Delta \mu$	Chemical potential	1 J
μ_l	Chemical potential for ice	$1 \frac{g}{cm^3}$
μ_s	Chemical potential for water	$1 \frac{5}{\text{cm}^3}$
ϱ_l	Density	$1 \frac{g}{cm^3}$ $1 \frac{g}{cm^3}$ $1 \frac{g}{cm^3}$
ϱ_l	Density of liquid water	$1 \frac{g}{cm^3}$

Density of ice

 ϱ_{ice}

Dimensionless quantities

2 menoromeso quantities		
β	Mean squared displacement of	
	sodium and chloride ions	
ε	Thickness of transition layer	
ζ	Length	
ζ_b	Inflection point of order	
	parameter $\eta(\zeta_b) = \frac{1}{2}$	
ζ_c	Critical length	
$\frac{\zeta_c}{\bar{\zeta}}$	Wave variable	
η	Order parameter	
$\Delta\Theta$	Applied temperature difference	
κ	Wave number	
κ_c	Critical wave number	
$\frac{\kappa_c}{\hat{\lambda}}$	Eigenvalue	
ρ	Radius of nucleus	
$ ho_c$	Critical radius	
ρ_a	Length at $\Delta G_{tot} = 0$	
σ	Salinity	
$ar{\sigma}$	Mean of Salinity	
$arphi_{LG}$	Landau–Ginzburg free energy	
	density	
$arphi_L$	Landau free energy density	
$arphi_G$	Ginzburg free energy density	
$oldsymbol{\Phi}_{LG}$	Landau-Ginzburg free energy	
$oldsymbol{\Phi}_L$	Landau free energy	
Φ_G	Ginzburg free energy	
τ	Time	
$ au_0$	Time scaling factor	
$ au_1$	Parameter for time dependent	
	coefficient β	
d	Parameter for time dependent	
	coefficient β	
\bar{c}	Constant freezing velocity	
m	Temperature dependent driving	
	force parameter	
N	Number of water molecules	
P	Porosity	

one-dimensional problem because it is sufficient to consider the radius. He adopted a quartic free energy density-order parameter relationship published by Harrowell and Oxtoby [39]. We extend Kobayashi's approach by adding a salinity flow. We divide the article into timeindependent and time-dependent processes and try to find a connection between phase field and classical nucleation theory in Section 4.3. Similar to Grandi [40] we use the Landau–Ginzburg theory [41]. With the assumption that salt is a passive tracer which does not undergo a phase transition we avoid the 4th derivation according to Cahn-Hilliard [42]. In the following we considers one-dimensional boundaries. In this paper we designate the transition layers as kinks [43,44] according to Appendix A.3. This one-dimensional approach is suitable to be extended to higher dimensions (see Fig. 1) as well as to sea water. A special focus of the present work will be stability of the appearing kink distribution in dependence of sea water salinity. The thickness of the boundary layers corresponds to the double critical radius of a nucleus and is found to be the length of five hexagons (see Fig. 2). The article is divided into three main sections: "Time-independent processes" (Section 2), "Time-dependent processes" (Section 3), and "Numerical solutions" (Section 4). Section 4 connects time-independent irreversible thermodynamic processes with the time-dependent phase field theory and extends the Kobayashi model with a salinity equation.

 $0.917 \frac{g}{cm^3}$

2. Time-independent processes

2.1. Phase field approach

The Landau–Ginzburg free energy density $\varphi_{LG}(\eta)=\varphi_L(\eta)+\varphi_G(\eta)$ is composed of the Landau free energy density φ_L and the Ginzburg term of free energy density φ_G . In the three-dimensional case, the index "L" denotes the volume term or Landau potential and the index "G" refers to the gradient term introduced by Vitaly Ginzburg. A general description can be found in Chapter 13 in [45]. For a time-dependent consideration, the Landau–Ginzburg free energy is often referred to as the Lyapunov function in the mathematical literature. The Landau free energy density bases on the assumption, that the Gibbs free energy density can be expanded in a series about the order parameter $\eta(\zeta)$ [35]

$$\begin{split} \varphi_L(\eta(\zeta), m(\Delta\Theta)) &= \frac{1}{4} \eta^4 - \left(\frac{1}{2} - \frac{m}{3}\right) \eta^3 + \left(\frac{1}{4} - \frac{m}{2}\right) \eta^2 \\ &= \frac{1}{4} \eta^2 (\eta - 1)^2 + \frac{m}{3} \eta^3 - \frac{m}{2} \eta^2, \end{split} \tag{1}$$

with the order parameter $\eta(\zeta)$ as a function of the position ζ such as a driving force parameter $m(\Delta(\Theta))$ for phase transition

$$m(\Delta\Theta) = \frac{1}{2} \frac{\Delta T_0 - \Delta T}{\Delta T_0} = \frac{1}{2} (1 - \Delta\Theta), \qquad (2)$$

which determines the shape of the double well potential density φ_L depending on the temperature $\Delta T = T - T_s$ with the dimensionless temperature difference

$$\Delta\Theta = \frac{\Delta T}{\Delta T_0} = \frac{T - T_s}{T_0 - T_s},\tag{3}$$

where T_s is the lowest supercooling temperature that can be reached and T_0 the equilibrium temperature. A restriction of the Landau theory relates to the value of the order parameter $\eta(\zeta)$. This must be small enough for the development of the thermodynamic potential to be interrupted after the fourth order in η . The value of the order parameter changes with the temperature difference from the critical temperature. In order for the development to be valid this difference must be sufficiently small. In addition, the evolution coefficients must behave smoothly in the vicinity of the critical point, i.e. they must not become singular, so that the thermodynamic potential remains finite. We use the approach of Kobayashi, where the temperature dependence of the evolution coefficients are chosen such that the order parameter $\eta(\zeta)$ remains small enough, i.e. $\eta(\zeta) \leq 1$.

2.2. Phase boundary solutions

The double well potential is symmetrical because of m=0. Therefore we have two double zeros at $\eta(\zeta)=0$ and $\eta(\zeta)=1$. There is neither supercooling or overheating. The Landau free energy density $\varphi_L(\eta(\zeta),\eta_\zeta(\zeta))$ can be written

$$\varphi_{LG}(\eta, \eta_{\zeta}) = \varphi_L(\eta(\zeta), m) + \varphi_G(\eta_{\zeta}), \tag{4}$$

with the gradient term $\varphi_G = \frac{\varepsilon^2}{2} \eta_\zeta^2(\zeta)$. We denote $\frac{\partial \eta}{\partial \zeta} = \eta_\zeta$, $\frac{\partial \eta}{\partial \tau} = \eta_\tau$ etc. The coefficient ε determines the width of the transition regions between the domains and corresponds to the double critical radius of a stable nucleus. At the moment we consider only the symmetric double-well potential density, i.e. $\Delta\Theta=1$ or m=0. The part φ_L of the Landau–Ginzburg free energy density φ_{LG}

$$\varphi_{LG}(\eta, \eta_{\zeta}) = \underbrace{\frac{\varepsilon^2}{2} \left(\frac{\partial \eta}{\partial \zeta}\right)^2}_{\varphi_{C}} + \underbrace{\frac{1}{4} \eta^2 (\eta - 1)^2}_{\varphi_{L}}$$
(5)

possesses the double roots $\eta_0=0$ and $\eta_0=1$. If the variational action principle in Appendix A.1 according to dimensionless quantities

$$\delta \int_{\zeta_1}^{\zeta_2} \varphi_{LG}(\eta, \eta_{\zeta}) d\zeta = 0 \tag{6}$$

is applied to the free energy density, we obtain the Euler–Lagrange equation according to Eq. (A.1)

$$\frac{\partial \varphi_{LG}}{\partial \eta} - \frac{d}{d\xi} \frac{\partial \varphi_{LG}}{\partial \eta_r} = 0, \tag{7}$$

and subsequently

$$\frac{1}{2}\eta(\eta-1)(2\eta-1) - \varepsilon^2 \frac{\partial^2 \eta}{\partial \zeta^2} = \frac{\partial \varphi_L(\eta)}{\partial \eta} - \varepsilon^2 \frac{\partial^2 \eta}{\partial \zeta^2} = 0,$$
 (8)

with the solutions $\eta=0$, $\eta=\frac{1}{2}$ and $\eta=1$. Addition to the trivial solutions we search the first non trivial steady state solution for the phase field model. We also find a solution as a function of ζ . For this purpose Eq. (8) can be integrated with respect to integration by parts on the right hand side

$$\int \frac{\partial \varphi_L}{\partial \eta} \frac{\partial \eta}{\partial \zeta} d\zeta = \varepsilon^2 \int \frac{\partial^2 \eta}{\partial \zeta^2} \frac{\partial \eta}{\partial \zeta} d\zeta, \tag{9}$$

and obtain an expression analogous to the virial theorem

$$\varphi_L(\eta) = \underbrace{\frac{1}{2} \epsilon^2 \left(\frac{\partial \eta}{\partial \zeta}\right)^2}_{\varphi_C},\tag{10}$$

which reflects the conservation of energy. This fact will allow us to solve the static problem by quadrature

$$\zeta - \zeta_b = \varepsilon \int_{\eta(\zeta_b)}^{\eta(\zeta)} \frac{d\eta}{\sqrt{2\varphi_I(m=0)}} = \pm 2\sqrt{2}\varepsilon \tanh^{-1}(1-2\eta), \tag{11}$$

and obtain as a result of the quadrature, two solutions are obtained, a kink and an antikink according to the opposite choice of the sign([46])

$$\eta(\zeta) = \frac{1}{2} \left(1 \mp \tanh^{-1} \left(\frac{1}{4\varepsilon} \sqrt{2} (\zeta - \zeta_b) \right) \right) = \frac{1}{1 + \exp(\pm \frac{\sqrt{2}}{2\varepsilon} (\zeta - \zeta_b))}. \tag{12}$$

The static solution (12) corresponds to a zero-energy trajectory because of $\varphi_L - \varphi_G = 0$ as a result of the symmetry of the non linear double-well potential. The stationary solution $\eta(\zeta)$ in Eq. (12) can be designated as kink or antikink and is a sigmoid function where two states are also distinguished. Eq. (12) is not a solution to a classical linear wave equation (26). The order parameter $\eta(\zeta)$ can be seen as a quantitative relationship between the probabilities of the two states being occupied, $\eta(\zeta) > \frac{1}{2}$ (mostly ice) and $\eta(\zeta) < \frac{1}{2}$ (mostly water) in Fig. 3. The inflection point of the order parameter $\eta(\zeta)$ is determined by $\eta(\zeta = \zeta_b) = \frac{1}{2}$. An infinitely thin transition layer ($\varepsilon \to 0$)

$$\lim_{\epsilon \to 0} \frac{1}{1 + \exp\left(\frac{\sqrt{2}}{2\epsilon} \left(\zeta - \zeta_b\right)\right)} = \begin{cases} 0 & \text{for } \zeta > \zeta_b \\ \frac{1}{2} & \text{for } \zeta = \zeta_b \\ 1 & \text{for } \zeta < \zeta_b \end{cases}$$
 (13)

only separates the states $\eta=0$ and $\eta=1$. Until now, only boundary conditions could be defined that do not allow any predictions about the freezing velocity. Therefore, time-dependent processes will considered in Section 3. By means of the slope of the kink $\eta_{\zeta}(\zeta)$ determined by ε

$$\frac{\partial \eta(\zeta)}{\partial \zeta} = \mp \frac{1}{4\sqrt{2}\varepsilon} \operatorname{sech}^2\left(\frac{1}{4\varepsilon}\sqrt{2}(\zeta - \zeta_b)\right) \tag{14}$$

we obtain the corresponding stationary Landau–Ginzburg free energy density $\varphi_{LG}(\zeta)$

$$\varphi_{LG}(\zeta) = \varphi_G + \varphi_L = 2\varphi_G = 2\varphi_L = \varepsilon^2 \eta_\zeta^2(\zeta) = \frac{1}{32} \operatorname{sech}^4 \left(\frac{1}{4\varepsilon} \sqrt{2}(\zeta - \zeta_b) \right),$$
(15)

with the maximum $\varphi_L(\zeta=\zeta_b)=\frac{1}{32}.$ If we integrate Eq. (15) we get the Landau–Ginzburg free energy Φ_{LG}

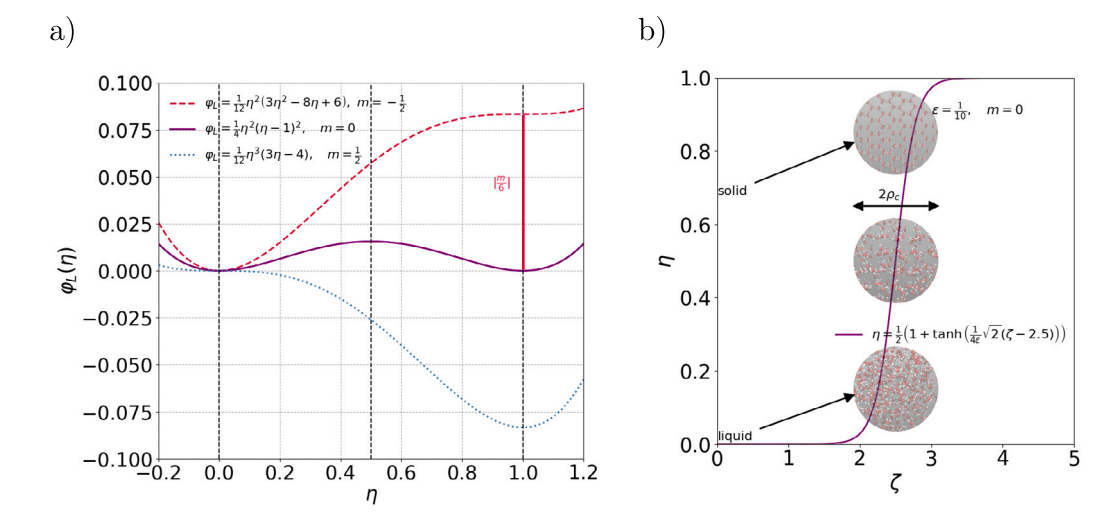


Fig. 3. (a) Maximal superheating (red) and supercooling (blue). (b) Interface of the thickness of the twice critical radius $\zeta_c = 2\rho_c$ with the critical length ζ_c . This length ζ_c is the shortest length as result of the stability analysis in Fig. 9 in Section 4.3 This length ζ_c results from the intersection point of the eigenvalue $\tau_0 \hat{\lambda}$ with the wave number axis κ , i.e. τ₀ λ = 0. Karim and Haymet [47] used a TIP4P water model to calculate the oxygen density profile during a melting process. Gránásy [38] adopted this molecular dynamics simulation for its approach. The transition region between solid and liquid corresponds to the length ζ_c . The melting process of ice (TIP3P-water model [48]) from solid state to liquid state was carried out using a molecular dynamic simulation.

$$\Phi_{LG} = \int_{-\infty}^{\infty} \varphi_{LG}(\zeta) d\zeta
= \frac{\varepsilon}{24\sqrt{2}} \tanh\left(\frac{\zeta - \zeta_b}{2\sqrt{2}\varepsilon}\right) \left(\cosh\left(\frac{\zeta - \zeta_b}{\sqrt{2}\varepsilon}\right) + 2\right) \operatorname{sech}^2\left(\frac{\zeta - \zeta_b}{2\sqrt{2}\varepsilon}\right) \Big|_{-\infty}^{\infty}
= \frac{\sqrt{2}\varepsilon}{12}.$$
(16)

A sharp interface boundary is associated with a small Landau free energy density and consequently with a small Landau free energy. The order parameter $\eta(\zeta, m = 0)$ in Eq. (12), the free energy density $\varphi_I(\zeta, m=0)$ in Eq. (15) and the free energy $\Phi_I(\zeta, m=0)$ in Eq. (16) are solutions for the stationary case.

3. Time-dependent processes

For the time-dependent non-equilibrium case, we consider the Landau–Ginzburg free energy Φ_{LG} as a function of an time and space dependent order parameter $\eta(\tau,\zeta)$. The dynamics of the order parameter is described by the time dependent Landau-Ginzburg theory (TDLG

$$\tau_0 \frac{\partial \eta(\tau, \zeta)}{\partial \tau} = -\frac{\delta \Phi_{LG}}{\delta \eta} = -\eta^3 + \left(\frac{3}{2} - m\right) \eta^2 - \left(\frac{1}{2} - m\right) \eta + \varepsilon^2 \frac{\partial^2 \eta(\tau, \zeta)}{\partial \zeta^2}$$
$$= \eta \left(\eta - 1\right) \left(-\eta + \frac{1}{2} - m\right) + \varepsilon^2 \frac{\partial^2 \eta(\tau, \zeta)}{\partial \zeta^2}, \tag{17}$$

with the dimensionless time $\tau = \frac{t}{t_0}$. Here $\tau_0 = \frac{t_1}{t_0}$ denotes a dimensionless time factor. The right side of the TDLG equation results from a variation derivative. The time-dependent term $\tau_0 \frac{\partial \eta}{\partial \tau}$ is not a

result of the variation and was only postulated. To introduce the parameter "time" for a irreversible process, an additional assumption is needed [49] sketched in Appendix A.5. At this point it should be noted that the jump of η at the freezing point, which characterizes a first-order phase transition, is missing because there is no root of η that can become complex for any m. We used a spectral method in order to solve the time-dependent partial differential equation. For this purpose we use the so-called exponential time differencing scheme of second order (ETD2) [50] described in Appendix A.2. The periodic boundary conditions are ensured by a "Fast Fourier Transformation" (FFT).

3.1. Propagating wave front solutions of the TDLG equation for $|m| \leq \frac{1}{2}$

If a travelling wave front exists it can be written in the form $\eta(\zeta, \tau) =$ $\bar{\eta}(\bar{\zeta})$ with $\bar{\zeta} = \zeta + \bar{c}\tau$, where \bar{c} is the wave speed. Substituting the travelling wave form into Eq. (17), $\bar{\eta}(\bar{\zeta})$ satisfies

$$\frac{\varepsilon^{2}}{\tau_{0}} \frac{d^{2}\bar{\eta}(\bar{\zeta})}{d\bar{\zeta}^{2}} - \bar{c}\bar{\eta}_{\bar{\zeta}} + \frac{1}{\tau_{0}} \underbrace{\bar{\eta}\left(\frac{1}{2} - m - \bar{\eta}\right)(\bar{\eta} - 1)}_{-\Pi(\bar{\eta})}$$

$$= \frac{\varepsilon^{2}}{\tau_{0}} \frac{d^{2}\bar{\eta}(\bar{\zeta})}{d\bar{\zeta}^{2}} - \bar{c}\bar{\eta}_{\bar{\zeta}} + \frac{1}{\tau_{0}} \underbrace{\left(\bar{\eta}(\bar{\eta} - 1)\left(\frac{1}{2} - \bar{\eta}\right) + m(1 - \bar{\eta})\bar{\eta}\right)}_{-\Pi(\bar{\eta})} = 0. \tag{18}$$

Because of the fixed phase relationship $\bar{\zeta} = \zeta + \bar{c}\tau$, the partial differential equation (17) is reduced to an ordinary differential equation. The drift term $\bar{c}\bar{\eta}_{\bar{\zeta}}$ is associated with a running wave front with a constant velocity \bar{c} . If the velocity $\bar{c}=0$, Eq. (18) is reduced to the stationary case (8). The fixed phase relation condition allows a reversible motion in the reverse direction, if we replace τ by $-\tau$ or \bar{c} by $-\bar{c}$. The function $\Pi(\bar{\eta})$ possesses two zeros as fixed points, zero and one and a movable zero within the interval [0,1] dependent on m. The part of the polynomial $\Pi(\bar{\eta})$ that includes the coefficient m must be equal to the drift term $\bar{c}\bar{\eta}_{\bar{c}}(\bar{\zeta})$

$$\pm \frac{d\bar{\eta}(\bar{\zeta})}{d\bar{\zeta}} = \pm \frac{m}{\tau_0} \bar{\eta}(\bar{\eta} - 1) \tag{19}$$

if we want to get a wave with a constant speed. The differential equation (19) can be integrated immediately

$$\bar{\eta}_{\pm}(\bar{\zeta}) = \frac{1}{2} \left(1 \mp \tanh \left(\frac{m}{2\bar{c}\tau_0} \left(\bar{\zeta} - \bar{\zeta}_b \right) \right) \right), \tag{20}$$

if $\bar{\eta}(\bar{\zeta} = \bar{\zeta}_b) = \frac{1}{2}$. Comparing solutions (20) and (12) in consideration of $\zeta - \zeta_b = \bar{\zeta} - \bar{\zeta}_b$, the wave velocity \bar{c} follows from $\frac{m}{2\bar{c}\tau_0} = \frac{\sqrt{2}}{4\epsilon}$, so that

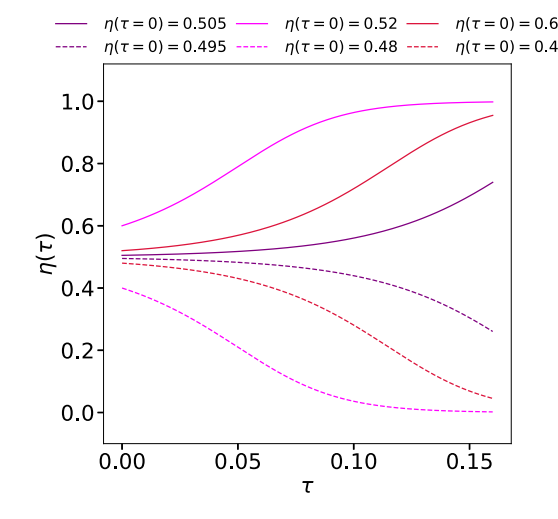
$$\bar{c} = \sqrt{2} \frac{\varepsilon}{\tau_0} m = \frac{\sqrt{2}}{\varepsilon} m \tag{21}$$

because of $\tau_0 = \varepsilon^2$. From Eq. (19) one obtains a Lagrange function $\mathcal L$

$$\mathcal{L}(\bar{\eta}, \bar{\eta}_{\bar{\zeta}}) = \frac{1}{2}\bar{c}^2 \left(\frac{\partial \bar{\eta}(\bar{\zeta})}{\partial \bar{\zeta}}\right)^2 - \frac{1}{2}\frac{m^2}{r_0^2}\bar{\eta}^2(\bar{\zeta})\left(\bar{\eta}(\bar{\zeta}) - 1\right)^2 = 0. \tag{22}$$

as a result of the fixed phase relation. If one uses the fixed phase relationship $\bar{\zeta} = \zeta + \bar{c}\tau$, then the following relationships also apply $\frac{\partial \eta(\zeta,\tau)}{\partial \zeta} = \frac{\partial \bar{\eta}(\bar{\zeta})}{\partial \bar{\zeta}} \frac{\partial \bar{\zeta}}{\partial \zeta} = \frac{\partial \bar{\eta}(\bar{\zeta})}{\partial \bar{\zeta}}$ and $\frac{\partial \eta(\zeta,\tau)}{\partial \tau} = \frac{\partial \bar{\eta}(\bar{\zeta})}{\partial \zeta} \frac{\partial \bar{\zeta}}{\partial \tau} = \bar{c} \frac{\partial \bar{\eta}(\bar{\zeta})}{\partial \bar{\zeta}} = \bar{c} \frac{\partial \eta(\zeta,\tau)}{\partial \zeta}$ so that

$$\mathcal{L}(\eta, \eta_{\tau}) = \frac{1}{2} \left(\frac{\partial \eta(\tau, \zeta)}{\partial \tau} \right)^2 - \frac{1}{2} \frac{m^2}{\tau_0^2} \eta^2(\zeta, \tau) \left(\eta(\zeta, \tau) - 1 \right)^2 = 0.$$
 (23)



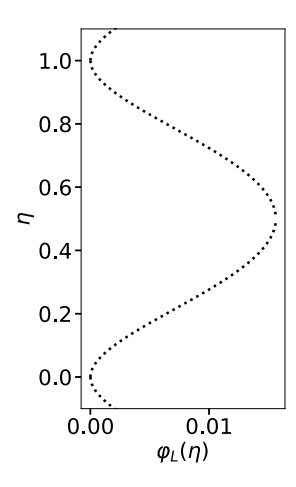


Fig. 4. A slight disturbance in the initial conditions of Eq. (32) determines which of the two states is reached. The trajectories run into one of the two minima at different times of the double well $\varphi_L(\eta)$ of Eq. (5). If the initial conditions are chosen as random variable, the behaviour is similar to the stochastic Weidlich model [51] and can therefore serve as a basis for coupling to a stochastic model.

Using the virial theorem (10) for τ satisfying the fixed phase relation, $4\varphi_L(\eta,\tau)=2\varepsilon^2\eta_\zeta^2(\zeta,\tau)=\eta^2(\zeta,\tau)\left(\eta(\zeta,\tau)-1\right)^2$ and $2m^2=\varepsilon^2\bar{c}^2$ as well as $\tau_0=\varepsilon^2$ one finally obtains

$$\mathcal{L}(\eta_{\zeta},\eta_{\tau}) = \frac{1}{2} \left(\frac{\partial \eta(\tau,\zeta)}{\partial \tau} \right)^{2} - \frac{\bar{c}^{2}}{2} \left(\frac{\partial \eta(\tau,\zeta)}{\partial \zeta} \right)^{2}. \tag{24}$$

The Euler-Lagrange equation

$$\frac{\partial \mathcal{L}(\eta_{\zeta}, \eta_{\tau})}{\partial \eta} - \frac{d}{d\zeta} \frac{\partial \mathcal{L}(\eta_{\zeta}, \eta_{\tau})}{\partial \eta_{\zeta}} - \frac{d}{d\tau} \frac{\partial \mathcal{L}(\eta_{\zeta}, \eta_{\tau})}{\partial \eta_{\tau}} = 0$$
 (25)

yields a wave equation

$$\bar{c}^2 \frac{\partial \eta^2(\tau, \zeta)}{\partial \zeta^2} - \frac{\partial \eta^2(\tau, \zeta)}{\partial \tau^2} = 0, \tag{26}$$

that is satisfied

$$\eta(\zeta, \tau) = \frac{1}{2} \left(1 \mp \tanh \left(\frac{1}{2\sqrt{2\varepsilon}} \left(\zeta + \bar{c}\tau \right) \right) \right)$$
(27)

according to the solution (20) if $\bar{\zeta}$ is replaced by $\zeta+\bar{c}\tau$ and $\bar{\zeta}_b=0$. Eq. (27) solves the wave equation (26) because of the fixed phase relationship $\bar{\zeta}=\zeta+\bar{c}\tau$ in contrast to Eq. (12). While in Eq. (17) the temporal derivative has only been postulated, the temporal derivative in the wave equation (26) is also obtained from a variational problem. Due to the fixed phase relationship, Eq. (27) is a topological reversible solution, which is also reflected in the symmetry of the wave equation (26). There is no specific direction of time for this propagating wave. Translocated position of the stationary solution by $\bar{c}\tau$ due to velocity \bar{c} satisfies the condition of the zero-energy trajectory in Eq. (12) or (18) with the boundary conditions $\lim_{\bar{\zeta}\to\infty}\bar{\eta}_+(\bar{\zeta})=0$ and $\lim_{\bar{\zeta}\to\infty}\bar{\eta}_+(\bar{\zeta})=1$ or $\lim_{\bar{\zeta}\to\infty}\bar{\eta}_-(\bar{\zeta})=1$ and $\lim_{\bar{\zeta}\to\infty}\bar{\eta}_-(\bar{\zeta})=0$. Because the shape of the travelling wave front does not change, the gradient part of the Landau free energy density φ_G remains invariant and consider only the Landau part φ_L

$$\tau_0 \frac{\partial \eta(\tau)}{\partial \tau} = -\varphi_L(\eta) = \eta (\eta - 1) \left(-\eta + \frac{1}{2} \right). \tag{28}$$

This can be transformed into a Bernoulli differential equation. Then we shift η by $\frac{1}{2}$, i.e. $\eta = \bar{\eta} + \frac{1}{2}$ and get

$$\tau_0 \frac{d\bar{\eta}(\bar{\zeta})}{d\bar{\zeta}} = -\bar{\eta}^3 + \frac{1}{4}\bar{\eta},\tag{29}$$

which can be converted into a linear differential equation

$$\tau_0 \frac{\partial u}{\partial \tau} + \frac{1}{2}u = 2 \tag{30}$$

by substitution $u = \frac{1}{n^2}$, with the solution

$$u(\tau) = C \exp\left(-\frac{\tau}{2\tau_0}\right) + 4. \tag{31}$$

Let us substitute again u in $\bar{\eta}$ and $\bar{\eta}$ in η and choose the initial condition $\eta(\tau=0)=\eta_a$, we get the final solution

$$\eta(\tau) = \frac{1}{2} \pm \frac{1}{\sqrt{4 + \left(\frac{1}{\left(\eta_a - \frac{1}{2}\right)^2} - 4\right) \exp\left(-\frac{\tau}{2\tau_0}\right)}}.$$
 (32)

The closer the initial conditions are to the phase transition point $\eta=\frac{1}{2}$, the later the two states $\eta=0$ and $\eta=1$ in Fig. 4 are reached. The time to reach a steady state is proportional to the square of the width of the transition layer ε . Furthermore, if ε is proportional to the size of a critical nucleus, the nucleation rate $\frac{1}{\tau_0}$ becomes smaller, because larger nuclei are required to prevent that these nuclei decay again.

4. Irreversible time-dependent numerical solutions for freezing processes

4.1. Freezing of fresh water

The time dependent Eq. (17) describes a nucleation and isotropic growth during the freezing. Between the dimensioned velocity c and the dimensionless velocity \bar{c} exists the relationship

$$c = \frac{z}{t} = \frac{z_0}{t_0} \frac{\zeta}{\tau} = \frac{z_0}{t_0} \bar{c} = \frac{z_0}{t_0} \sqrt{2m} \frac{\varepsilon}{\tau_0}.$$
 (33)

for a constant velocity at a constant temperature, i.e. m=const. This method is used to determine t_0 if z_0 is known. The width of the liquid–solid interface can be determined from a remelting process and this length z_0 we use as a scaling factor. A arbitrary parameter z_1 allows us to choose the dimensionless thickness of interface $\varepsilon=\frac{1}{z_0}z_1$ in such a way that the numerical problem is well-conditioned. Therefore, ε is the well-conditioned width of the liquid–solid interface. From the chemical potential

$$\Delta\mu = \frac{q(T-T_0)}{T_0} = \frac{\Delta\gamma}{\varrho_l}\frac{\partial f}{\partial z_0}$$

and the specific interfacial potential [52,53]

$$f(z_0) = \frac{z_0^2}{z_0^2 + h^2}$$

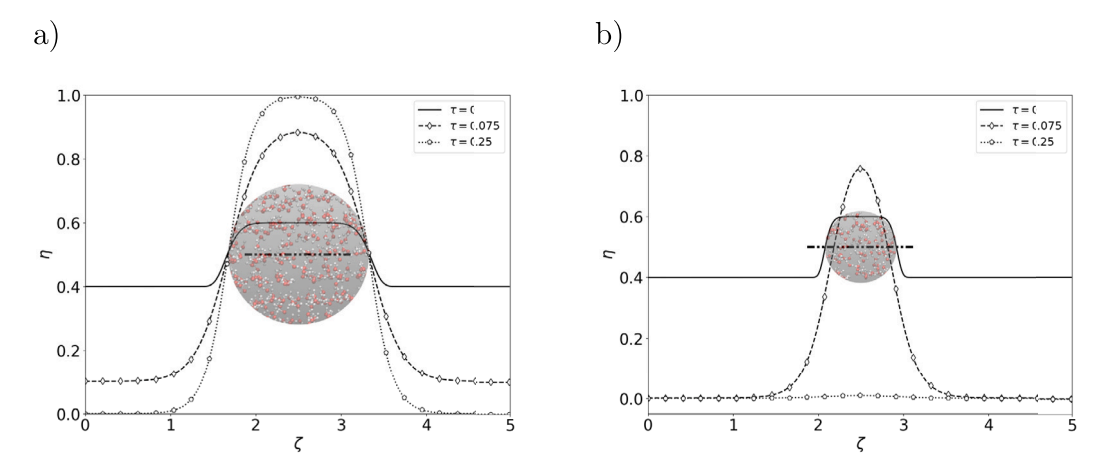


Fig. 5. Time dependent evolution (a) for a successful nucleation process if $\Delta \zeta > \zeta_c$ or $\Delta \rho > \rho_c$ and (b) for an unsuccessful nucleation process if $\Delta \zeta < \zeta_c$ or $\Delta \rho < \rho_c$ at the phase transition point. Initial conditions: $\eta(\zeta, \tau = 0) = \frac{4}{10} + \frac{2}{10} \exp\left(-\frac{1}{5}(1.4(\zeta - 2.5))^8\right)$ (successful), $\eta(\zeta, \tau = 0) = \frac{4}{10} + \frac{2}{10} \exp\left(-\frac{1}{5}(2.8(\zeta - 2.5))^8\right)$ (unsuccessful) for $\epsilon = \frac{1}{10}$, m = 0.

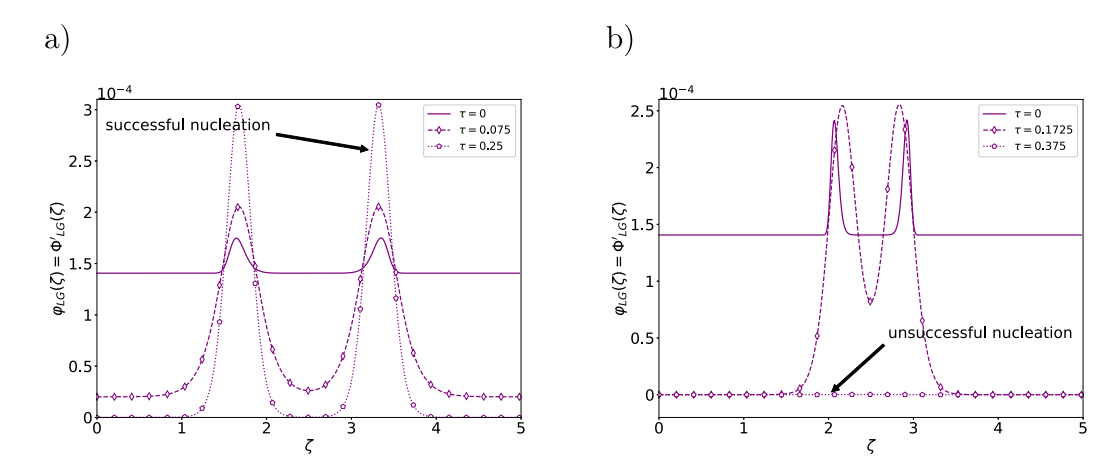


Fig. 6. Time dependent development of the Landau-Ginzburg free energy density corresponds to Fig. 5. The transition layers disappear in case (b).

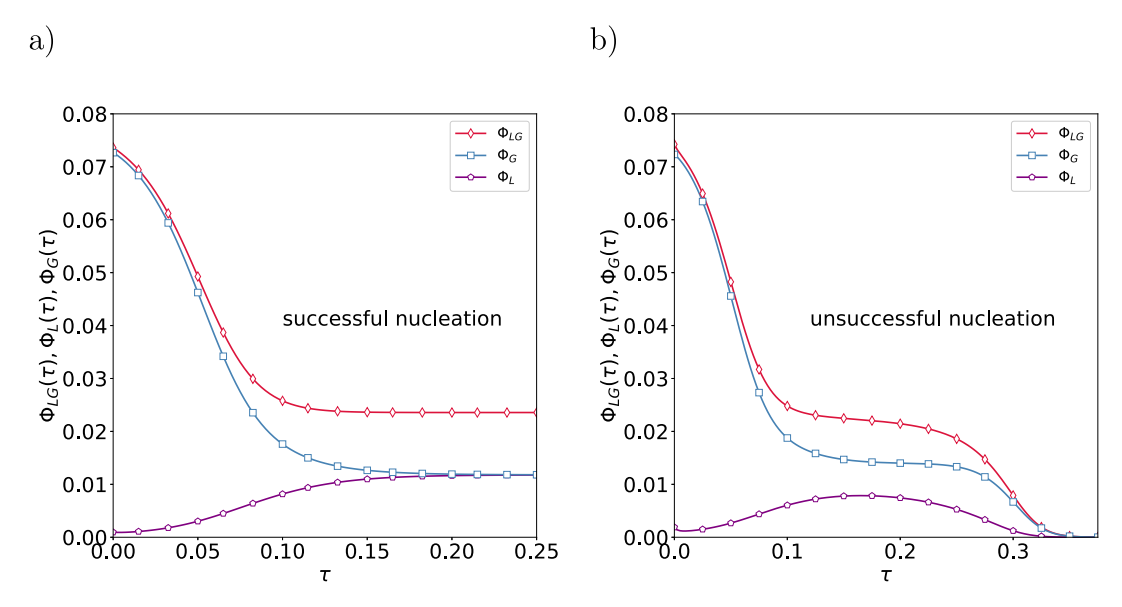


Fig. 7. (a) Because of the virial theorem (10) we have $\Phi_L = \Phi_G$ in the stationary case. (b) The Landau–Ginzburg energy disappears.

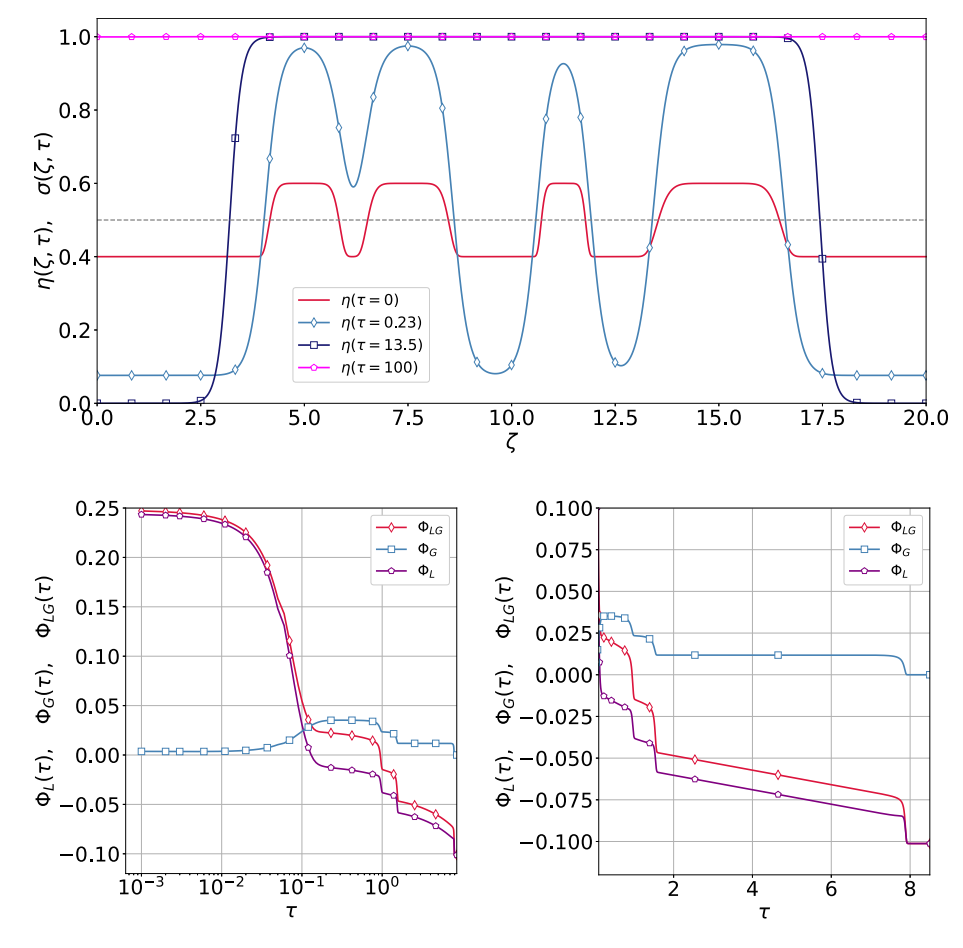


Fig. 8. The initial formation of the phase boundaries leads to an increase in the gradient term while the Landau free energy decreases during the freezing process. Initial conditions and parameter: $\eta(\tau=0,\zeta)=0.4+\frac{1}{5}\exp\left(-\frac{1}{5}\left(\frac{7}{5}(\zeta-5)\right)^8\right)+\frac{1}{5}\exp\left(-\frac{1}{5}\left(\frac{6}{5}\left(\zeta-\frac{15}{2}\right)\right)^8\right)+\frac{1}{5}\exp\left(-\frac{1}{5}\left(\frac{11}{5}\left(\zeta-\frac{45}{4}\right)\right)^8\right)+\frac{1}{5}\exp\left(-\frac{1}{5}\left(\frac{4}{5}(\zeta-15)\right)^8\right), d=3, \ \tau_1=0.3, \ \beta=\frac{1}{48m}, \ \tau_0=\varepsilon^2=\frac{1}{100}, \ T_0=273.15 \ \text{K}, \ T_1=236.6 \ \text{K}, \ T_2=236.6 \ \text{K}, \ T=270.93 \ \text{K}.$

results

$$\frac{(h^2+z_0^2)^2}{z_0}=\frac{2h^2\Delta\gamma}{\varrho_l\Delta\mu}.$$

The long-range potentials fall off quadratically with distance similar to the van der Waals equation, in which the attractive pressure is proportional to the square of the particle density. With $h \ll z_0$, i.e. $h^2 + z_0^2 \approx z_0^2$ can be estimated the layer thickness for a remelting process [53]

$$z_0 = \left(-\frac{2h^2\Delta\gamma T_0}{\varrho_I q(T_0 - T)}\right)^{\frac{1}{3}}.$$
 (34)

The surface tension $\Delta\gamma=\gamma_{lv}+\gamma_{sl}-\gamma_{sv}$ is composed of various interfaces, liquid-vapour, solid-liquid and solid-vapour, ϱ_l is the density of the liquid and h a constant of the order of a molecular spacing. The distance h can be interpreted as an expression, which contributes to a non-negligible residual volume according to the van der Waals equation. More measurements at the interface were carried out by Beaglehole et al. [54,55] and Dosch et al. [56,57] and Furukawa et al. [58]. Besides the known measured values $T_0=273.15$ K, $T-T_0=20$ mK [59, 60], $\Delta\gamma=6.64$ $\frac{\rm erg}{\rm cm^2}$ [53], $\varrho_l=0.99$ $\frac{\rm g}{\rm cm^3}$, $q=3.33\cdot10^9$ $\frac{\rm erg}{\rm g}$, the value for the molecular distance h still remains undetermined. For this, an interval between 2.77 Å and 4.52 Å could be chosen according to Fig. 2. For h=2.89 Å this gives a layer thickness of $z_0=2.84$ nm, approximately one order of magnitude greater than the molecular distance h. With these values, the layer thickness z_0 coincides with the double critical radius $2r_c$. The second scaling factor $t_0=z_0\frac{c}{c}$ can be determined from the freezing velocity c. The forming wurtzite structure of hexagonal ice

prefers the growth perpendicular to the c axis in the c-plane (Fig. 2). The different growth rates are based on the observation that only twomolecular groups are needed to build up the c-plane in contrast to the a-plane, where four-molecular groups are needed and the probability of the occurrence of the four-molecular group is much smaller than for the two-molecular group [60,61]. For this reason, different empirical relationships are given for the growth rates according to the growth direction [60]. With a supercooling of 20 mK there is a freezing velocity of $c = \frac{1}{2} \frac{\mu m}{s}$ perpendicular to the c-axis [7], (Fig. 9.10 in [60]) and therefore a scaling factor $t_0 = z_0 \frac{\bar{c}}{c} = z_0 \frac{1}{c} \sqrt{2m \frac{\epsilon}{\tau_0}}$. A supercooling of 20 mK corresponds to m = 0.00027359 and we get $t_0 = 0.02197$ ms with $\epsilon^2 = \tau_0 = \frac{1}{100}$. First, we consider only the nucleation process without growth in which we consider only the nucleation process without growth, i.e. without a propagation of the wave front, $\bar{c} = 0$ in Fig. 5, Fig. 6 and Fig. 7. Initially, the nucleus radius $\rho(\tau=0)$ is larger than the critical radius $\rho_c=\frac{1}{2}\zeta_c$. A stable nucleus develops without a subsequent growth process. For $\tau\to\infty$ a state of a dynamic equilibrium between a melting and a freezing process is reached and the nucleation is completed. The gradient term of the Landau free energy $\Phi_G(\tau)$ does not decrease over the entire time. This stabilizes the structure in this open system. Because the Landau-Ginzburg free energy $\Phi_{LG}(au)$ no longer changes, the second phase, the growth is missing. In contrast to Fig. 5a, the radius $\rho(\tau = 0)$ of the nucleus in Fig. 5b is less than the critical radius ρ_c . The nucleus does develop to a maximum size, but then it decays because the critical radius ρ_c is not reached and is not exceeded although $\Delta\Theta = 1$ has been set. We remark, that the free energy ΔG_{tot} of the classical nucleation theory in Section 4.2 describes only the free energy of the nucleus without an additional environment. This is different, however, in the case of the phase field model where we

integrate the Landau free energy over the entire system. The gradient component of the Landau free energy $\Phi_G(\tau)$ is always smaller than or equal to the potential component $\Phi_L(\tau)$ because only the nucleation, i.e. m=0, is considered. In the next step we could assume arbitrary initial conditions in the vicinity of $\eta=0$. A certain freezing time is necessary until the critical phase transition point $\eta=0.5$ is reached. We start the simulation in the vicinity of the phase transition point $\eta=0.5$ in Fig. 8 because the first time period is not interesting for the structure formation. During the freezing process, more and more boundary layers disappear. Each loss of a boundary layer means a jump in the Landau-Ginzburg free energy in Fig. 8. During the freezing fronts spread, the Ginzburg term of the free energy Φ_G does not change, the Landau term Φ_L decreases.

4.2. Classical nucleation theory

The classical nucleation theory considers the Gibbs free energy ΔG which is composed of a bulk and a surface term. For the homogeneous nucleation one obtains an equation for the Gibbs free energy barrier $\Delta G_{tot}(r) = \Delta G(r) + 4\pi r^2 \gamma = N\Delta \mu + 4\pi r^2 \gamma$ and therefore

$$\Delta G_{tot} = -\frac{4}{3}\pi r^3 \Delta g_v + \underbrace{4\pi r^2 \gamma}_{\text{volume term}} = -\frac{4}{3}\pi r^3 \frac{N}{V} \Delta \mu + 4\pi r^2 \gamma, \tag{35}$$

with the Gibbs free energy density $\Delta g_v = \frac{\Delta G}{V}$, the volume $V = \frac{4}{3}\pi r^3$, the number of molecules N, the radius r, the chemical potential $\Delta \mu = \mu_l - \mu_s$ as difference between the liquid and solid state and the interfacial tension γ between two phases. The necessary condition $\Delta G'(r) = 0$ determines the critical radius $r = r_c = \frac{2\gamma}{4g_v} = \frac{2\gamma}{2\mu} \frac{V}{N}$ at the maximum of the Gibbs free energy $\Delta G_c = \frac{16}{3}\pi \frac{\gamma^3}{(\Delta g_v)^2}$ for the smallest stable nucleus. Similar to the approach of Mori et al. [62] we assume that the relation $N\Delta\mu = \Delta G = \Delta H - T\Delta S \approx \Delta H - T\frac{\Delta H}{T_0} = \Delta H \left(1 - \frac{T}{T_0}\right)$ is also valid approximately at the first-order phase transition, where $T = T_s$ denotes the deepest supercooling temperature, T_0 the freezing temperature, T_0 the entropy and T_0 the Helmholtz free energy (enthalpy). Using the density of ice φ_{lce} with $\varphi_{lce}V = nM_{\rm H_2O}$ for n=1 mol and the specific enthalpy (latent heat or heat of fusion) T_0 0 and T_0 1 the critical radius T_c 1 in the framework of the Gibbs–Thomson equation for an isotropic sphere can be written in the form

$$r_c = \frac{2\gamma T_0}{\varrho_{ice} q(T_0 - T_s)} \tag{36}$$

for $T = T_s < T_0$ with the Gibbs free energy

$$\Delta G_c = \frac{16}{3} \pi \gamma^3 \frac{T_0^2}{\varrho_{ice}^2 q^2 (T_0 - T_s)^2}.$$
 (37)

The number of molecules N in the critical nucleus is the ratio of the total volume divided by the volume of one molecule

$$N(r_c) = \frac{V}{\frac{V_m}{N_A}} = \frac{\frac{4}{3}\pi r_c^3}{\frac{V_m}{N_A}} = \frac{32}{3}\pi \gamma^3 \frac{T_0^3}{(T_0 - T_s)^3 \varrho_{ice}^3 q^3} \frac{N_A}{V_m},$$
 (38)

with the Avogadro constant N_A and the molar volume of water V_m . For a first-order phase transition, a critical radius $r_c=1.42$ nm at the maximum of the Gibbs free energy $\Delta G_c=2.45\cdot 10^{-12}$ erg is calculated with the measured values $\gamma=29\,\frac{\rm erg}{\rm cm^2}$, $\varrho=\varrho_{ice}=0.917\,\frac{\rm g}{\rm cm^3}$, $\varrho=3.33\cdot 10^9\,\frac{\rm erg}{\rm g}$, $T_0=273.15$ K and $T_s=236.6$ K. This critical nucleus contains N=401 molecules with the molar volume of water $V_s=18\,\frac{\rm cm^3}{\rm cm^3}$. The

N=401 molecules with the molar volume of water $V_m=18\,{\rm {cm^3}\over {mol}}$. The contributions from the surface and volume term are equal if $\Delta G(r)=0$. At this point the nucleus has the radius

$$r_a = \frac{3\gamma}{\Delta g_v} = \frac{3\gamma V}{N\Delta\mu} = \frac{3\gamma T_0}{\varrho_{ice}q(T_0 - T_s)},\tag{39}$$

or $r_a=\frac{3}{2}r_c$. We use the relationships $r=r_0\rho$ and $r_a=r_0\rho_a$ in order to introduce the dimensionless radius ρ and ρ_a and obtain from Eq. (35)

$$\Delta G_{tot}(\rho) = 4\pi \gamma r_0^2 \rho^2 \left(1 - \frac{\rho}{\rho_a} \right),\tag{40}$$

with $2r_0 = z_0$.

4.3. Bridge between phase field and classical nucleation theory

The relation between the critical length and the critical radius $\zeta_c=2\rho_c$ connects the phase field theory with the classical nucleations theory. Then the double critical radius $2\rho_c$ from classic nucleation theory should be equal to the critical length $\zeta_c=\frac{2\pi}{\kappa_c}$. Here κ_c designed the largest possible wave number in the TDLG equation if m=0, i.e. $\Delta(\Theta)=1$. The critical value κ_c is determined by a linear stability analysis by introducing small perturbations $\tilde{\eta}=\eta-\eta_0$ in Eq. (17) for m=0 and obtain the linearized TDGL equation

$$\tau_0 \frac{\partial \widetilde{\eta}(\tau, \zeta)}{\partial \tau} = \left(-\frac{1}{2} + 3\eta_0 - 3\eta_0^2 \right) \widetilde{\eta} + \varepsilon^2 \frac{\partial^2 \widetilde{\eta}(\tau, \zeta)}{\partial \zeta^2}. \tag{41}$$

Using the Fourier ansatz $\tilde{\eta} = \exp(\hat{\lambda}\tau + \lambda\zeta) = \exp(\hat{\lambda}\tau + i\kappa\zeta)$, where $\lambda = i\kappa$ with the wave number $\kappa = \frac{2\pi}{\zeta}$, we find

$$\tau_0 \hat{\lambda} = -\frac{1}{2} + 3\eta_0 (1 - \eta_0) - \varepsilon^2 \kappa^2. \tag{42}$$

Only if the eigenvalues $\hat{\lambda}$ in a certain range of wave numbers κ are larger than zero, structures can arise. This condition is fulfilled by the fixed point $\eta_0 = \frac{1}{2}$

$$\tau_0 \hat{\lambda} = \frac{1}{4} - \varepsilon^2 \kappa^2. \tag{43}$$

The other two fixed points $\eta_0=0$ and $\eta_0=1$ are therefore excluded. The critical wave number κ_c is obtained for $\widehat{\lambda}=0$. With $\varepsilon=\frac{1}{10}$ we have $\kappa=\kappa_c=\frac{1}{2\varepsilon}=\frac{2\pi}{\zeta_c}=\frac{2\pi}{2\rho_c}=5$ and thus $\rho_a=\frac{3}{2}\rho_c=\frac{3}{10}\pi$. An ice structure can only arise if $\kappa\leq\kappa_c$ or $\rho_c\leq\rho$. With respect to Eq. (16) we set $\gamma=\gamma_0\Phi_G=\gamma_0\frac{\Phi_{LG}}{2}=\gamma_0\frac{\sqrt{2}}{24}\varepsilon$ and obtain from Eq. (40)

$$\frac{\Delta G_{tot}(\rho)}{\gamma_0 r_0^2} = 4\pi \frac{\sqrt{2}}{24} \varepsilon \rho^2 \left(1 - \frac{\rho}{\rho_a} \right). \tag{44}$$

The scaling parameters $\gamma_0 = \frac{24}{\sqrt{2}\epsilon} \gamma$ and $r_0 = \frac{5}{\pi} r_c = \frac{5}{\pi} \frac{2\gamma T_0}{\rho q(T_0 - T_c)}$ can

be obtained with respect to Eqs. (16) and (36). The critical length of the phase field theory can be identified with the critical radius of the classical nucleation theory in Fig. 9. This is the unique point where we can find a connection between phase field theory and equilibrium thermodynamics in the time independent thermodynamics equilibrium. In the following Section, the critical radii and the interfacial tensions are compared with the simulations at the molecular level.

4.4. Comparison of the total Gibbs free energy ΔG_{tot} with free energy calculations of TIP4P model of H_2O

In contrast to the phenomenological classical nucleation and growth theory, molecular dynamics and Monte Carlo methods use partition functions of a Einstein reference crystal for the calculation of the free energy [63-65]. Because an interfacial tension is not explicitly considered in this concept, only the total Gibbs free energy can be compared with each other. Vlot et al. [65] performed a Monte Carlo Simulation of a 4-site transferable intermolecular potential (TIP4P) model with N = 576 molecules and calculated for this grand canonical ensemble a molar Gibbs free energy 54.9 $\frac{\text{kJ}}{\text{mol}}$, i.e. $\Delta G_{tot} = 9.11 \cdot 10^{-13} \, \text{erg}$ for an ice nucleus. The Gibbs free energy for an ice nucleus of 578 molecules is $2.32 \cdot 10^{-12}$ erg for an interfacial tension of $29 \frac{\text{erg}}{\text{cm}^2}$ shown in Fig. 10 on the left side. We consider only the right intersection point for the successful nucleation because the second intersection point does not form an ice nucleus. We overestimate the Gibbs free energy more than double compared to the Monte Carlo simulation. In order to achieve the same Gibbs free energy, the interfacial tension must be reduced to $\gamma = 24.65 \frac{\text{erg}}{\text{cm}^2}$ according to the right side of Fig. 10. The experimentally determined values for the interfacial tension for liquid water-ice γ vary from 15 $\frac{\text{erg}}{\text{cm}^2}$ to 32 $\frac{\text{erg}}{\text{cm}^2}$ [60]. This interfacial tensions

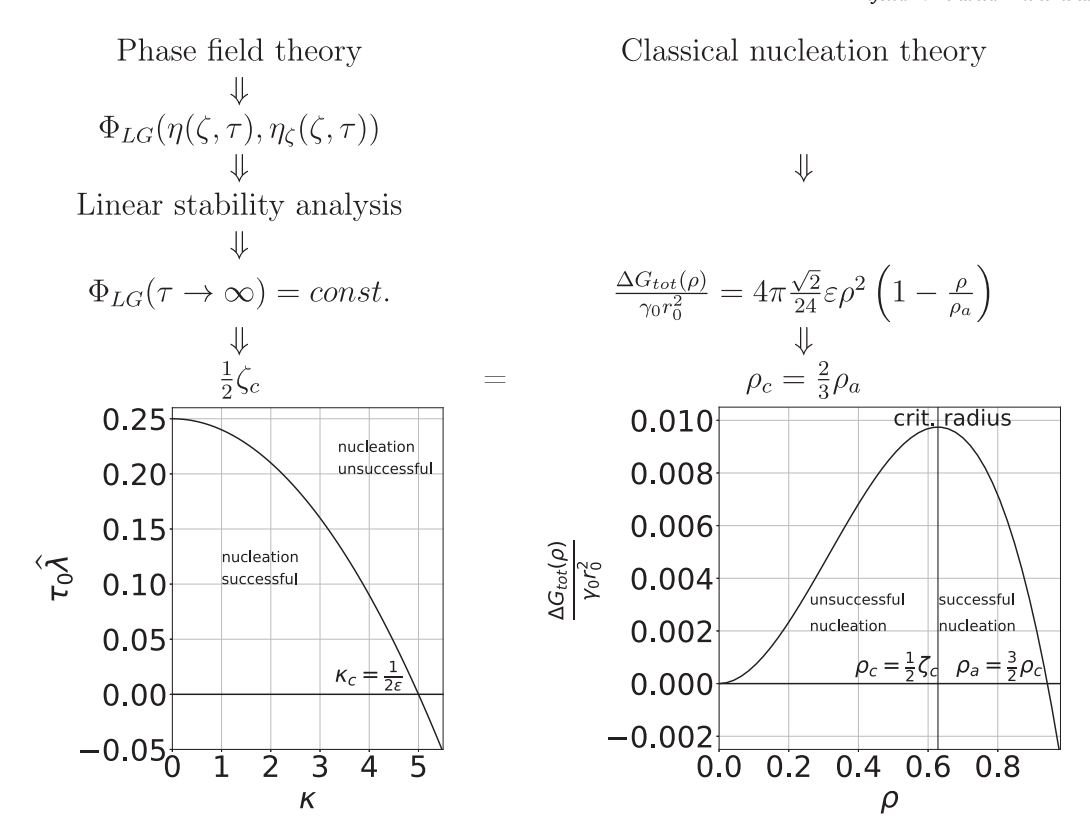


Fig. 9. Comparison between phase field theory and classical nucleation theory for estimation of critical nucleus: $\zeta_c = \frac{2\pi}{\kappa_c} = 2\rho_c$ with $\varepsilon = \frac{1}{10}$ and $\rho_c = \frac{\pi}{5}$. The double critical radius ρ_c is equal to the critical length ζ_c , because the classical nucleation theory determines critical radii in contrast to the stability analysis of phase field theory, which determines the total length. The critical length ζ_c is the length for the eigenvalue $\tau_0 \hat{\lambda} = 0$ and the critical radius is determined from the maximum of Gibbs free energy.

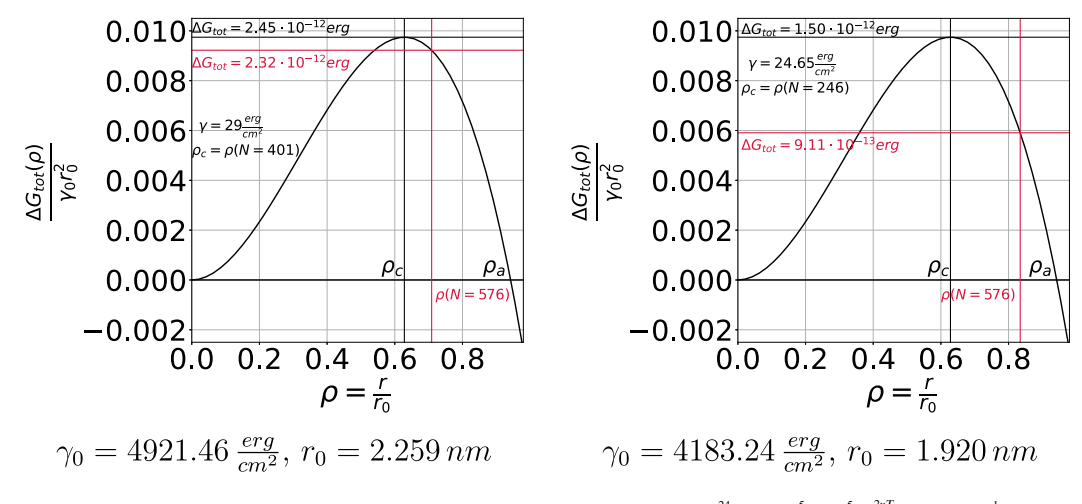


Fig. 10. Influence of the interfacial tension on the Gibbs free energy with $\gamma_0 = \frac{24}{\sqrt{2}\epsilon}\gamma$, $r_0 = \frac{5}{\pi}r_c = \frac{5}{\pi}\frac{2\gamma T_0}{eq(T_0-T_s)}$ and $\varepsilon = \frac{1}{10}$.

determine the critical radii from $r_c(N=55)=0.73\,\mathrm{nm}$ to $r_c(N=538)=1.57\,\mathrm{nm}$ with the corresponding number of molecules N from 55 to 538. Unfortunately, the TIP4P water model underestimates the melting temperature between 230 K and 250 K and overestimates the density of ice between 0.942 $\frac{\mathrm{g}}{\mathrm{cm}^3}$ and 0.963 $\frac{\mathrm{g}}{\mathrm{cm}^3}$ [65]. As long as the range of interfacial energy cannot be narrowed down more, the question of the most plausible interfacial energy has to remain unanswered.

4.5. Freezing in seawater

For the description of seawater we extend the Landau–Ginzburg functional for fresh water Φ_{LG} by interaction between salt and ice. The

Ginzburg–Landau function used in this manuscript subsumes a possible mixing entropy for salt in the coupling terms $\sigma\eta^2$ and $\sigma\eta^3$. This is a simplifying assumption compared to the description in [40] and follows for seawater by considering the entropy of mixing

$$\sigma \ln \sigma + (1 - \sigma \ln(1 - \sigma)$$

in the regime $\sigma\ll 1$. In this regime, the second term is unimportant. At $\sigma=0$, the term $\sigma\ln\sigma$ is an indeterminate form $0\times\infty$. For the description of the regime $\sigma\ll 1$ (seawater), we therefore apply the L'Hospital rule:

$$\lim_{\sigma \to 0} (-\sigma \ln \sigma) = -\lim_{\sigma \to 0} \frac{(\ln \sigma)'}{(1/\sigma)'} = -\lim_{\sigma \to 0} \frac{1}{\sigma} \left(-\sigma^2 \right) = \lim_{\sigma \to 0} \sigma,$$

and replace $\sigma \ln \sigma$ by σ . The linear shift m by $\frac{1}{2}\sigma$ describes a freezing point depression due to the colligative property of salt in Eq. (45) correspond to Appendix A.4

$$\varphi_{LG} = \underbrace{\frac{1}{4}\eta^4 - \left(\frac{1}{2} - \frac{1}{3}\left(m - \frac{1}{2}\sigma\right)\right)\eta^3 + \left(\frac{1}{4} - \frac{1}{2}\left(m - \frac{1}{2}\sigma\right)\right)\eta^2 + \frac{\beta}{2}\sigma^2}_{\varphi_L} + \underbrace{\frac{1}{2}\epsilon^2 \left(\frac{\partial\eta}{\partial\zeta}\right)^2}_{}.$$
(45)

The dimensionless salinity scaled to the maximal supercooling because of Eq. (2) is $\sigma = \frac{i \cdot K_F}{-\Delta T_0} s$ with the cryoscopic constant $K_F = -1.853 \frac{\text{K kg}}{\text{mol}}$ of NaCl in water, the van't Hoff-factor i = 2 for NaCl and the universal gas constant *R*. The expression $\Delta T_0 = T_0 - T_s$ designates the temperature difference between the freezing point T_0 and the maximal supercooling temperature T_s of pure water. The mean salinity of the oceans is approximately $s=0.598 \, \frac{\text{mol}}{\text{kg}}$ or 35 $\frac{g}{\text{kg}}$ and leads to a freezing point depression of $K_F \cdot is = -\frac{RT_0^2}{g} \cdot is = -\frac{RT_0^2 n M_{\text{H}_2\text{O}}}{\Delta H} \cdot is = -\frac{RT_0 n M_{\text{H}_2\text{O}}}{\Delta S} \cdot is = -2.2 \, \text{K}$ as result of the Clausius–Clapeyron relation valid only for low concentrations. According to the mole fraction $x=\frac{35}{1000} \, \frac{n_{\text{H}_1\text{on}2\text{O}}}{n_{\text{NaCl}}} = \frac{n_{\text{H}_2\text{O}}}{n_{\text{NaCl}}} = \frac{n_{\text{H}_2\text{O}}}{n_{\text{N}_2\text{O}}} = \frac{n_{\text{H}_2\text{O}}}{n_{\text{N}_2\text{O$

0.0107 contain approximately 100 H₂O molecules 1 NaCl molecule, also $1Na^+$ ion and 1 Cl⁻. The value of β determines the width of the salinity distribution similar to diffusion constant. The parameter β can be determined from the condition that $\sigma = 0$ for $\eta = 1$ in the equilibrium case. This condition can be satisfied only as long as everything does not thaw or freeze, because salinity σ is a conserved quantity. Analogous to the potentials in thermodynamics the Landau-Ginzburg potential density φ_{LG} guarantee the equality $\frac{\partial^2 \varphi_{LG}}{\partial \eta \partial \sigma} = \frac{\partial^2 \varphi_{LG}}{\partial \sigma \partial \eta}$ for the existence of a total differential. The functional derivatives yield the evolution

$$\begin{split} \tau_0 \frac{\partial \eta(\tau,\zeta)}{\partial \tau} &= -\frac{\delta \varPhi_{LG}}{\delta \eta} = -\frac{\partial \varPhi_L}{\partial \eta} + \varepsilon^2 \frac{\partial^2 \eta(\tau,\zeta)}{\partial \zeta^2} \\ &= -\eta^3 + \left(\frac{3}{2} - \left(m - \frac{1}{2}\sigma\right)\right) \eta^2 - \left(\frac{1}{2} - \left(m - \frac{1}{2}\sigma\right)\right) \eta \\ &+ \varepsilon^2 \frac{\partial^2 \eta(\tau,\zeta)}{\partial \zeta^2} \\ &= \eta(1 - \eta) \left(\eta - \frac{1}{2} + m - \frac{1}{2}\sigma\right) + \varepsilon^2 \frac{\partial^2 \eta(\tau,\zeta)}{\partial \tau^2}, \end{split}$$

$$\tau_0 \frac{\partial \sigma(\tau, \zeta)}{\partial \tau} = -\frac{\partial^2}{\partial r^2} \frac{\delta \Phi_{LG}}{\delta \sigma} = -\varepsilon^2 \frac{\partial^2}{\partial r^2} \left(\frac{1}{3} \frac{1}{2} \eta^3 - \frac{1}{4} \eta^2 - \beta \sigma \right). \tag{47}$$

The operator $-\epsilon^2 \frac{\partial^2}{\partial r^2}$ leads to a continuity equation with the salinity as a conserved quantity. Eq. (47) has a character of a Cahn-Hilliard equation without the 4th derivative of the order parameter or salinity. We would obtain such a type of equation for the salinity if we replace $\frac{\beta}{2}\sigma^2$ with a Ginzburg energy density $\frac{1}{2}\beta\left(\frac{\partial\sigma}{\partial\zeta}\right)^2$ for the salinity in Eq. (45). However, it was not absolutely necessary to consider the fourth derivative for a brine channel formation. The salinity flow is balanced by the opposite fluxes $-\frac{1}{6}\epsilon^2 \frac{\partial^2}{\partial \zeta^2} \eta^3$ and $\frac{1}{4}\epsilon^2 \frac{\partial^2}{\partial \zeta^2} \eta^2$. This flux is determined by the parameter β in Eq. (47). In the stationary case, this

$$\tau_0 \frac{\partial \sigma(\tau, \zeta)}{\partial \tau} = -\varepsilon^2 \frac{\partial^2}{\partial \zeta^2} \left(\frac{1}{6} \eta^3 - \frac{1}{4} \eta^2 - \beta \sigma \right) = 0 \tag{48}$$

can be integrated

$$0 = \frac{\partial}{\partial \zeta} \left(\frac{1}{6} \eta^3 - \frac{1}{4} \eta^2 - \beta \sigma \right) + C_1, \tag{49}$$

with $C_1 = 0$ if $\frac{\partial \eta}{\partial r} = \frac{\partial \sigma}{\partial r} = 0$. As a result of the second integration

$$0 = \frac{1}{6}\eta^3 - \frac{1}{4}\eta^2 - \beta\sigma + C_2 \tag{50}$$

the constant C_2 is determined from the condition $\sigma(\eta_{max}) = \sigma_{min}$ and obtain $C_2 = \beta \sigma_{min} + \eta_{max}^2 \left(\frac{1}{4} - \frac{1}{6} \eta_{max} \right)$ and therefore

$$0 = \eta^2 \left(\frac{1}{6} \eta - \frac{1}{4} \right) - \eta_{max}^2 \left(\frac{1}{6} \eta_{max} - \frac{1}{4} \right) - \beta(\sigma - \sigma_{min})$$
 (51)

For $\sigma = \sigma_{max}$ and $\eta = \eta_{min}$ we get

$$\beta = \frac{\eta_{min}^2 \left(\frac{1}{6}\eta_{min} - \frac{1}{4}\right) - \eta_{max}^2 \left(\frac{1}{6}\eta_{max} - \frac{1}{4}\right)}{\sigma_{max} - \sigma_{min}}.$$
Because the values $\eta_{min} = 0$ and $\eta_{max} = 1$ in the stationary case

 $\frac{\partial \eta}{\partial x} = 0$ be achieved

$$\eta_0 = \begin{cases}
0 = \eta_{min}, \\
\frac{1}{2} - m + \frac{1}{2}\sigma, \\
1 = \eta_{max}
\end{cases}$$
(53)

the parameter β is simplified to

$$\beta = \frac{1}{12(\sigma_{max} - \sigma_{min})}.\tag{54}$$

Should salt completely suppressed from the ice, i.e. $\sigma_{min} = 0$ then we

$$\beta = \frac{1}{12\sigma_{max}}. (55)$$

According to Eq. (46) or (53) the unstable fixed point $\eta_0 = \frac{1}{2}$ is reached if $\frac{1}{2}\sigma = m$ and obtain $\sigma\left(\eta = \frac{1}{2}\right) = 2m$. If we set $\eta_{max} = 1$ and $\sigma_{min} = 0$ in Eq. (51) then $\beta \sigma = \eta^2 \left(\frac{1}{6} \eta - \frac{1}{4} \right) + \frac{1}{12}$. Because of $\beta \sigma_{max} = \beta \sigma (\eta = 0) = \frac{1}{12}$ and $\beta \sigma(\eta = \frac{1}{2}) = \frac{1}{24}$ we find $\sigma_{max} = \sigma(\eta = 0) = 2\sigma\left(\eta = \frac{1}{2}\right) = 4m$ and

$$\beta = \frac{1}{12\sigma_{max}} = \frac{1}{48m}. (56)$$

Three cases can be distinguished:

(I)
$$\beta < \frac{1}{48m}$$
: $\sigma_{max} - \sigma_{min} > 2\bar{\sigma}$

(II)
$$\beta = \frac{1}{48m}$$
: $\sigma_{max} - \sigma_{min} = 26$

(III)
$$\beta > \frac{1}{48m}$$
: $\sigma_{max} - \sigma_{min} < 2\bar{\sigma}$

(I) $\beta < \frac{1}{48m}$: $\sigma_{max} - \sigma_{min} > 2\bar{\sigma}$ (II) $\beta = \frac{1}{48m}$: $\sigma_{max} - \sigma_{min} = 2\bar{\sigma}$ (III) $\beta > \frac{1}{48m}$: $\sigma_{max} - \sigma_{min} < 2\bar{\sigma}$ In case (I), the salinity becomes negative during the desalination of ice and remains negative. In case (II), the salinity becomes negative during the desalination of ice but becomes exactly 0 in the stationary state or if the nucleation process is complete and only a wave front is still propagating. Assuming condition (II), negative salinities can only occur initially during the nucleation phase. Case (III) is a necessary condition, that the salinity does remain non-negative during the entire process. In addition, a minimum threshold of β must also be exceeded. The consequence of this is that a residual salinity always remains in the ice. Alternatively, a time-dependent coefficient $\beta_1(\tau)$ of the kind

$$\lim_{\tau \to \infty} \beta(\tau) = \lim_{\tau \to \infty} \frac{d+1}{d + \exp\left(-\frac{\tau_1}{\tau}\right)} \frac{1}{48m}$$

could also be introduced with two suitable constants d and τ_1 in Fig. 11 that prevent the initial overshoot of the salinity into the negative range. After a certain cooling phase, spatial distribution of ordered phase could occur at the critical phase transition point $\eta = \frac{1}{2}$ as shown in Fig. 12.

The result from numerical integration of Eqs. (46) and (47) is shown in Fig. 12. On the left two growing nuclei merge, in the centre the critical radius is not reached and the nucleus decays again and on the right a wave front moves until the salinity slows down the freezing front. The fusion of phase boundaries and the disappearance of an unstable nucleus leads to jumps in free energy $\Phi_{LG},~\Phi_{L},~\Phi_{G}$ and porosity $P = 1 - \frac{solid\ volume}{complete\ volume}$ in Fig. 13. In contrast to fresh water in Fig. 8, the Landau free energy can also increase if the porosity increases due to the loss of an unstable nucleus at $\tau = 13.5$.

(46)

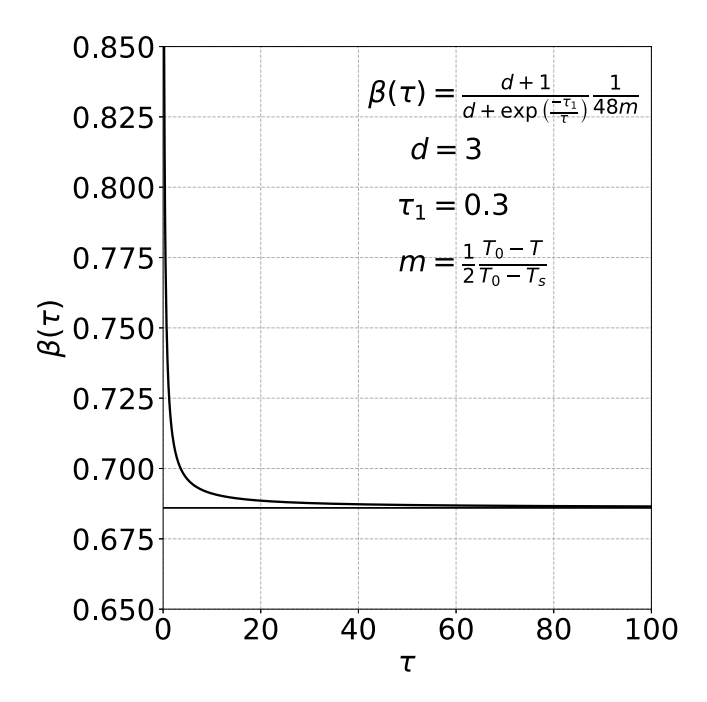


Fig. 11. The salinity flow is controlled by the time dependent coefficient β with $T_s = 236.6$ K, $T_0 = 273.15$ K, T = 270.93 K.

5. Summary and conclusion

For Kobayashi's time-dependent approach, a link to classical timeindependent classical nucleation theory is proposed. In a further step, salinity is introduced as a second field and Kobayashi's approach is extended. Without an alternating temperature field or an changing salinity field, the maximum of the eigenvalue $\tau_0 \hat{\lambda}$ in Fig. 9 is assigned to wave number $\kappa = 0$, that means, the wave length $\lambda \to \infty$. The frozen areas are not completely desalinated because flux in ice $-\frac{1}{6} \varepsilon^2 \eta_{\zeta\zeta}^3$ is opposed by a flux out from ice $\frac{1}{4}\epsilon^2\eta_{rr}^2$ including in Eq. (47). The parameter β is determined by the condition that the salinity is positive. In the steady state this can be done by integrating of Eq. (48) for suitable boundary conditions for the salinity. For the approach to the steady state we introduce the time dependent $\beta(\tau)$ that always fulfils the condition $0 \le \sigma \le \sigma_{max}$ at each ζ . In our extended Kobayashi approach the structure size is limited by a salinity profile that develops during the ice growth. This approach described the growth of the ice domain at small supercooling in connection with the salinity equation in difference to [42]. Furthermore, we used our enhanced model in order to simulate the fusion of the ice domains. The fusion of ice domains reduce the number of phase boundaries. This results in jumps of the Landau-Ginzburg energy at the time of domain fusions. The salinity-dependent isotropic approach can be extended with respect to different growth rates in different directions, resulting in anisotropic growth [66,67].

CRediT authorship contribution statement

Bernd Kutschan: Writing – original draft, Conceptualization. Silke Thoms: Writing – original draft, Supervision, Funding acquisition, Conceptualization. Andrea Thom: Conceptualization. Raghav Pathak: Conceptualization. Tim Ricken: Funding acquisition, Conceptualization.

Declaration of competing interest

The authors declare no conflict of interest.

Acknowledgement and founding sources

The authors are deeply indebted K. Kiesel for photographic picture of a freezing soap bubble (Fig. 1(b)). We thank the Deutsche Forschungsgemeinschaft (DFG, German Research Foundation, Germany) for supporting this work via the following projects: 463296570 (Priority Programme SPP 1158, Antarctica: TH 744/7-1); 312860381 (Priority Program SPP 1886, Subproject 12); 504766766 (Project Hybrid MOR). We acknowledge support by the Open Access publication fund of Alfred Wegener Institute Helmholtz Centre for Polar and Marine Research, Germany.

Appendix

A.1. First variation - one dimension

The variation of the functional $F_{LG}[\eta, s] = \int_{z_1}^{z_2} f_{LG}(z, \eta, \eta_z) dz$ yields

$$\begin{split} \delta F_{LG}[\eta] &= \delta \int_{z_1}^{z_2} f_{LG}(s,\eta,\eta_z) dz = \int_{z_1}^{z_2} \delta f_{LG}(s,\eta,\eta_z) dz \\ &= \int_{z_1}^{z_2} \left(\frac{\partial f_{LG}}{\partial \eta} \delta \eta + \frac{\partial f_{LG}}{\partial \eta_z} \delta \eta_z \right) dz, \end{split}$$

and the integration by parts

$$\begin{split} \int_{z_{1}}^{z_{2}} \frac{\partial f_{LG}}{\partial \eta_{z}} \delta \eta_{z} dz &= \delta \int_{z_{1}}^{z_{2}} \frac{\partial f_{LG}}{\partial \eta_{z}} \eta_{z} dz \\ &= \delta \left(\left[\frac{\partial f_{LG}}{\partial \eta_{z}} \eta \right]_{z_{1}}^{z_{2}} - \int_{z_{1}}^{z_{2}} \frac{d}{dz} \frac{\partial f_{LG}}{\partial \eta_{z}} \eta dz \right) \\ &= \underbrace{\left[\frac{\partial f_{LG}}{\partial \eta_{z}} \delta \eta \right]_{z_{1}}^{z_{2}} - \delta \int_{z_{1}}^{z_{2}} \frac{d}{dz} \frac{\partial f_{LG}}{\partial \eta_{z}} \eta dz}_{=0} \\ &= - \int_{z_{1}}^{z_{2}} \frac{d}{dz} \frac{\partial f_{LG}}{\partial \eta_{z}} \delta \eta dz. \end{split}$$

Hence becomes

$$\delta F_{LG}[\eta] = \delta \int_{z_1}^{z_2} f_{LG}(\eta,\eta_z) dz = \int_{z_1}^{z_2} \left(\frac{\partial f_{LG}}{\partial \eta} - \frac{d}{dz} \frac{\partial f_{LG}}{\partial \eta_z} \right) \delta \eta dz,$$

or the first variation

$$\frac{\delta}{\delta\eta}F_{LG}[\eta] = \frac{\partial f_{LG}}{\partial\eta} - \frac{d}{dz}\frac{\partial f_{LG}}{\partial\eta_z}.$$
(A.1)

The first variation of the Landau–Ginzburg free energy density f_{LG}

$$f_{LG}(\eta, \eta_z) = \underbrace{\frac{1}{4}\eta^4 - \left(\frac{1}{2} - \frac{m}{3}\right)\eta^3 + \left(\frac{1}{4} - \frac{m}{2}\right)\eta^2}_{f_I} + \underbrace{\frac{z_1^2}{2}\left(\frac{\partial\eta}{\partial z}\right)^2}_{C}, \tag{A.2}$$

with $m(\Delta T) = \frac{1}{2} \frac{\Delta T_0 - \Delta T}{\Delta T_c}$ yields corresponding to Eqs. (A.1)

$$\begin{split} t_1 \frac{\partial \eta(t,z)}{\partial t} &= -\frac{\delta F_{LG}}{\delta \eta} = -\frac{\partial f_{LG}}{\partial \eta} + \frac{d}{dz} \frac{\partial f_{LG}}{\partial \eta_z} \\ &= -\eta^3 + \left(\frac{3}{2} - m\right) \eta^2 - \left(\frac{1}{2} - m\right) \eta + z_1^2 \frac{\partial^2 \eta(t,z)}{\partial z^2} \\ &= \eta(1 - \eta) \left(\eta - \frac{1}{2} + m\right) + z_1^2 \frac{\partial^2 \eta(t,z)}{\partial z^2}. \end{split} \tag{A.3}$$

Here η represents the order parameter, $\Delta T = T - T_s$ the temperature difference between the current temperature T and the supercooling temperature T_s with the equilibrium temperature T_0 , the space variable z and the time t. The corresponding greek letters denote the dimensionless quantities, linked by scaling factors z_0 and t_0 , that means $z = z_0 \zeta$ and $t = t_0 \tau$. We have to do

$$\frac{\partial \eta}{\partial \tau} = \frac{\partial \eta}{\partial t} \frac{\partial t}{\partial \tau}$$
$$\frac{\partial \eta}{\partial \zeta} = \frac{\partial \eta}{\partial z} \frac{\partial z}{\partial \zeta}$$

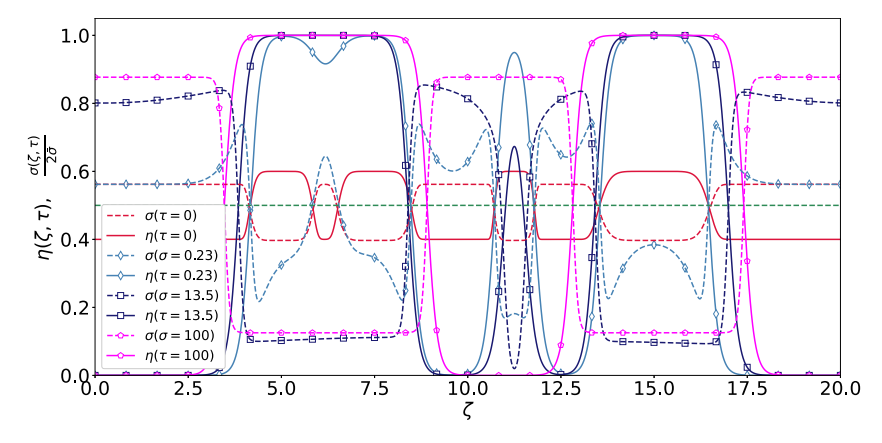
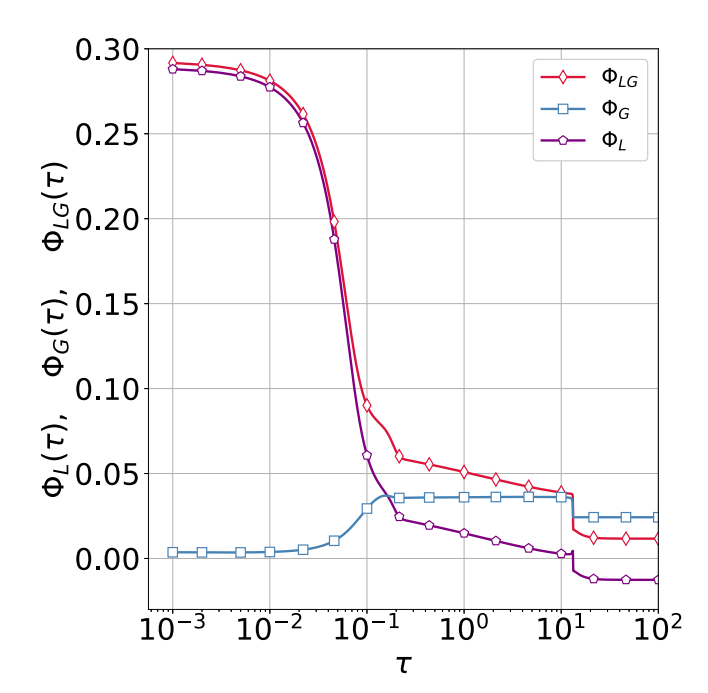


Fig. 12. In contrast to Fig. 8, the salinity here prevents the entire area from being frozen. Initial conditions and parameter: $η(τ = 0, ζ) = 0.4 + \frac{1}{5} \exp\left(-\frac{1}{5}\left(\frac{7}{5}(\zeta - 5)\right)^8\right) + \frac{1}{5} \exp\left(-\frac{1}{5}\left(\frac{6}{5}(\zeta - \frac{15}{2})\right)^8\right) + \frac{1}{5} \exp\left(-\frac{1}{5}\left(\frac{11}{5}(\zeta - \frac{45}{4})\right)^8\right) + \frac{1}{5} \exp\left(-\frac{1}{5}\left(\frac{4}{5}(\zeta - 15)\right)^8\right), σ(τ = 0, ζ) = \frac{1}{10}(1 - η(τ = 0, ζ)) + 0.0081, d = 3, τ_1 = 0.3, τ_0 = ε^2 = \frac{1}{100}, T_0 = 273.15 \text{ K}, T_s = 236.6 \text{ K}, T = 270.93 \text{ K}, ⟨σ⟩ = 0.0606.$



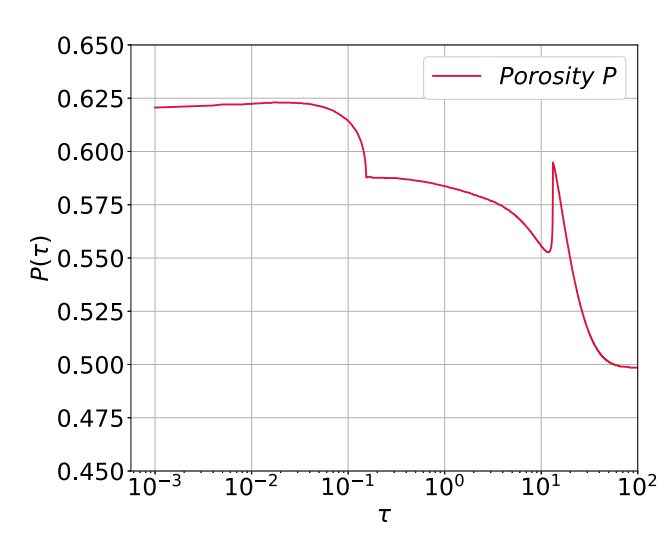


Fig. 13. The porosity increases immediately when a unstable nucleus disappears. This correlates with the increase of Landau free energy Φ_L .

$$\frac{\partial^2 \eta}{\partial \zeta^2} = \frac{\partial^2 \eta}{\partial z^2} \left(\frac{\partial z}{\partial \zeta} \right)^2 + \frac{\partial \eta}{\partial z} \underbrace{\frac{\partial^2 z}{\partial \zeta^2}}_{Q\zeta^2},$$

and obtain with $\frac{\partial \eta}{\partial t} = \frac{1}{t_0} \frac{\partial \eta}{\partial \tau}$, $\frac{\partial \eta}{\partial z} = \frac{1}{z_0} \frac{\partial \eta}{\partial \zeta}$, $\frac{\partial^2 \eta}{\partial z^2} = \frac{1}{z_0^2} \frac{\partial^2 \eta}{\partial \zeta^2}$ the equation

$$\frac{t_1}{t_0} \frac{\partial \eta(\tau, \zeta)}{\partial \tau} = -\eta^3 + \frac{3}{2} \eta^2 - m\eta^2 - \frac{1}{2} \eta + m\eta + \frac{z_1^2}{z_0^2} \frac{\partial^2 \eta(\tau, \zeta)}{\partial \zeta^2},$$
 (A.4)

and choose for example

$$\begin{split} \frac{t_1}{t_0} &= \tau_0, \\ \frac{z_1^2}{z_0^2} &= \varepsilon^2. \end{split}$$

In Eq. (A.4), z_1 and t_1 are scaling parameters. Therefore, we can set $\frac{\varepsilon^2}{\tau_0}=1$ without loss of generality. The factors t_0 and z_0 are determined from experimental values in Section 4.1. and do not depend on t_1 and z_1 . Because t_1 and z_1 are free parameters, we can set $\varepsilon^2=\tau_0$, which also avoids numerical instabilities of an ill-conditioned problem. Accordingly is

$$\begin{split} \tau_0 \frac{\partial \eta(\tau,\zeta)}{\partial \tau} &= -\eta^3 + \left(\frac{3}{2} - m\right) \eta^2 - \left(\frac{1}{2} - m\right) \eta + \varepsilon^2 \frac{\partial^2 \eta(\tau,\zeta)}{\partial \zeta^2} \\ &= \eta (1 - \eta) \left(\eta - \frac{1}{2} + m\right) + \varepsilon^2 \frac{\partial^2 \eta(\tau,\zeta)}{\partial \zeta^2}, \end{split} \tag{A.5}$$

and the corresponding dimensionless Landau–Ginzburg free energy density φ_{IG}

$$\varphi_{LG}(\eta, \eta_{\zeta}) = \underbrace{\frac{1}{4}\eta^4 - \left(\frac{1}{2} - \frac{m}{3}\right)\eta^3 + \left(\frac{1}{4} - \frac{m}{2}\right)\eta^2}_{\varphi_L} + \underbrace{\frac{1}{2}\varepsilon^2 \left(\frac{\partial\eta}{\partial\zeta}\right)^2}_{\varphi_G}.$$
 (A.6)

A.2. Exponential time differencing

Cox and Matthews [50] discussed several numerical iteration methods. We use the higher-order approximation for exponential time differencing method (ETD2) described by Eqs. (5) and (6) therein. The procedure is illustrated using Eq. (A.5). The real one-dimensional space is discretized and a reciprocal space is assigned to this space

$$\begin{split} \zeta &= \frac{L}{N} \left(0, 1, \dots, N-1 \right), & \text{real space} \\ \kappa &= \frac{2\pi}{L} \left(0, 1, \dots, \frac{N}{2} - 1, 0, -\frac{N}{2} + 1, \dots, -1 \right), & \text{reciprocal space} \end{split}$$

where N is the number of grid points and L is the total length. Eq. (17) must be transformed into reciprocal space by means of Fourier

transformation in order to be able to apply the iteration method

$$\mathcal{F}_{\tau(n+1)}(\eta(\zeta))(\kappa) = \underbrace{\mathcal{F}_{\tau(n)}(\eta(\zeta)) \exp(A\Delta\tau)}_{linear} + \underbrace{(f_1f_3)_{\tau(n)} + (f_2f_3)_{\tau(n-1)}}_{nonlinear},$$

with

$$A = -\frac{1}{\tau_0} \left(\frac{1}{2} - m \right) + \frac{\varepsilon^2}{\tau_0} (i\kappa)^2,$$

$$f_1 = \frac{(1 + A\Delta\tau) \exp(A\Delta\tau) - 1 - 2A\Delta\tau}{A^2 \Delta\tau},$$

$$f_2 = \frac{(-\exp(A\Delta\tau) + 1 + A\Delta\tau}{A^2 \Delta\tau},$$

$$f_3 = \frac{1}{\tau_0} \mathcal{F} \left(-\eta^3 + \left(\frac{3}{2} - m \right) \eta^2 \right) (\kappa).$$
(A.7)

In order to avoid indefinite expressions, the two limit values

$$\lim_{A \to 0} f_1 = \frac{3}{2} \Delta \tau,$$

$$\lim_{\Delta \to 0} f_2 = -\frac{1}{2} \Delta \tau$$

should be implied separately in the numerics. Finally, the inverse Fourier transform

$$\eta(\zeta) = \mathcal{F}^{-1}(\mathcal{F}_{\tau(n+1)}(\eta(\zeta))(\kappa))(\zeta)$$

yields the order parameter η in real space.

A.3. Instanton - kink - wavefront

The most general term is a "wavefront". We can adopt Rajaraman's intention that instantons are localized solutions of Euclidic field equations with finite Euclidian action [46]. In order to show that the solution of the time-independent Eq. (A.5)

$$\eta(1-\eta)\left(\eta - \frac{1}{2} + m\right) + \varepsilon^2 \frac{\partial^2 \eta}{\partial \zeta^2} = 0 \tag{A.8}$$

possesses the properties of an instanton, at least one corresponding time-dependent equation must exist. Eq. (A.8) should result from a suitable substitution of time of the time-dependent equation. The time-independent Eq. (A.8) for a static state can be obtained from a corresponding non linear time-dependent wave equation

$$\frac{1}{2}\varepsilon^2 \frac{\partial^2 \eta(\tau,\zeta)}{\partial \tau^2} - \frac{1}{2}\varepsilon^2 \frac{\partial^2 \eta}{\partial \zeta^2} = -\eta^3 + \left(\frac{3}{2} - m\right)\eta^2 - \left(\frac{1}{2} - m\right)\eta,\tag{A.9}$$

if we replace $\tau = -i\zeta$ we obtain Eq. (A.8).

A.4. Dimensionless equations with salinity - one dimension

The first variation of the Landau free energy density f_{LG}

$$f_{LG} = \underbrace{\frac{1}{4}\eta^4 - \left(\frac{1}{2} - \frac{1}{3}\left(m - \frac{1}{2}\sigma\right)\right)\eta^3 + \left(\frac{1}{4} - \frac{1}{2}\left(m - \frac{1}{2}\sigma\right)\right)\eta^2 + \frac{\beta}{2}\sigma^2}_{f_L} + \underbrace{\frac{z_1^2}{2}\left(\frac{\partial\eta}{\partial z}\right)^2}_{f_C}, \tag{A.10}$$

with $\sigma = \frac{1}{2} \frac{K_F i}{T_s - T_0} s$ and $m(\Delta T) = \frac{1}{2} \frac{\Delta T_0 - \Delta T}{\Delta T_0}$ yields corresponding to Eqs.

$$\begin{split} t_1 \frac{\partial \eta(t,z)}{\partial t} &= -\frac{\delta F_{LG}}{\delta \eta} = -\frac{\partial f_{LG}}{\partial \eta} + \frac{d}{dz} \frac{\partial f_{LG}}{\partial \eta_z} \\ &= -\eta^3 + \left(\frac{3}{2} - \left(m - \frac{1}{2}\sigma\right)\right)\eta^2 \\ &- \left(\frac{1}{2} - \left(m - \frac{1}{2}\sigma\right)\right)\eta + z_1 \frac{\partial^2 \eta(t,z)}{\partial z^2} \\ &= \eta(1-\eta)\left(\eta - \frac{1}{2} + m - \frac{1}{2}\sigma\right) + z_1 \frac{\partial^2 \eta t,z)}{\partial \zeta^2}, \end{split} \tag{A.11}$$

$$t_1 \frac{\partial \sigma(t,z)}{\partial t} &= -\frac{\delta F_{LG}}{\delta \sigma} = -\frac{\partial f_{LG}}{\partial \sigma} + \frac{d}{dz} \frac{\partial f_{LG}}{\partial \sigma}. \end{split}$$

$$=\frac{1}{6}\eta - \frac{1}{4}\eta - \beta\sigma\tag{A.12}$$

Here η represents the order parameter, $\Delta T = T - T_s$ the temperature difference between the current temperature T and the supercooling temperature T_s with the equilibrium temperature T_0 , s the molality of the salinity, K_F the cryoscopic constant, i the van't Hoff factor, z the space variable and t the time. The corresponding greek letters denote the dimensionless quantities, linked by scaling factors z_0 and t_0 , that means $z = z_0 \zeta$ and $t = t_0 \tau$. We have to do

$$\frac{\partial \tau}{\partial \sigma} = \frac{\partial t}{\partial \tau} \frac{\partial \tau}{\partial t},
\frac{\partial \sigma}{\partial \zeta} = \frac{\partial \sigma}{\partial t} \frac{\partial t}{\partial \tau},
\frac{\partial \eta}{\partial \zeta} = \frac{\partial \eta}{\partial z} \frac{\partial z}{\partial \zeta},
\frac{\partial^2 \eta}{\partial \zeta^2} = \frac{\partial^2 \eta}{\partial z^2} \left(\frac{\partial z}{\partial \zeta}\right)^2 + \frac{\partial \eta}{\partial z} \underbrace{\frac{\partial^2 z}{\partial \zeta^2}}_{=0},
\frac{\partial^2 \eta^2}{\partial \zeta^2} = 2 \left[\left(\frac{\partial \eta}{\partial z}\right)^2 \left(\frac{\partial z}{\partial \zeta}\right)^2 + \eta \underbrace{\frac{\partial^2 z}{\partial \zeta^2}}_{\partial \zeta^2} \right]$$

$$\frac{\partial^{2} \eta^{2}}{\partial \zeta^{2}} = 2 \left(\left(\frac{\partial \eta}{\partial z} \right)^{2} \left(\frac{\partial z}{\partial \zeta} \right)^{2} + \eta \underbrace{\frac{\partial^{2} z}{\partial \zeta^{2}}}_{=0} \underbrace{\frac{\partial \eta}{\partial z}}_{=0} + \eta \left(\frac{\partial z}{\partial \zeta} \right)^{2} \frac{\partial^{2} \eta}{\partial z^{2}} \right)$$

$$= 2 \left(\frac{\partial z}{\partial \zeta} \right)^{2} \underbrace{\left(\left(\frac{\partial \eta}{\partial z} \right)^{2} + \eta \frac{\partial^{2} \eta}{\partial z^{2}} \right)}_{\frac{1}{2} \frac{\partial^{2} \eta^{2}}{\partial z^{2}}},$$

$$\frac{\partial^{2} \eta^{3}}{\partial \zeta^{2}} = 3\eta \left(2\eta \left(\frac{\partial \eta}{\partial z} \right)^{2} \left(\frac{\partial z}{\partial \zeta} \right)^{2} + \eta \underbrace{\frac{\partial^{2} z}{\partial \zeta^{2}}}_{=0} \frac{\partial \eta}{\partial z} + \eta \left(\frac{\partial z}{\partial \zeta} \right)^{2} \frac{\partial^{2} \eta}{\partial z^{2}} \right)$$

$$= 3 \left(\frac{\partial z}{\partial \zeta} \right)^{2} \underbrace{\left(2\eta \left(\frac{\partial \eta}{\partial z} \right)^{2} + \eta^{2} \frac{\partial^{2} \eta}{\partial z^{2}} \right)}_{\frac{1}{3} \frac{\partial^{2} \eta^{3}}{\partial z^{2}}},$$

$$\frac{\partial^2 \sigma}{\partial \zeta^2} = \frac{\partial^2 \sigma}{\partial z^2} \left(\frac{\partial z}{\partial \zeta} \right)^2 + \frac{\partial \sigma}{\partial z} \underbrace{\frac{\partial^2 z}{\partial \zeta^2}}_{=0},$$

and obtain with $\frac{\partial \eta}{\partial t} = \frac{1}{t_0} \frac{\partial \eta}{\partial \tau}$, $\frac{\partial \sigma}{\partial t} = \frac{1}{t_0} \frac{\partial \sigma}{\partial \tau}$, $\frac{\partial \eta}{\partial z} = \frac{1}{z_0} \frac{\partial \eta}{\partial \zeta}$, $\frac{\partial^2 \eta}{\partial z^2} = \frac{1}{z_0^2} \frac{\partial^2 \eta}{\partial \zeta^2}$, $\frac{\partial^2 \eta}{\partial z^2} = \frac{1}{z_0^2} \frac{\partial^2 \eta}{\partial \zeta^2}$, $\frac{\partial^2 \eta}{\partial z^2} = \frac{1}{z_0^2} \frac{\partial^2 \eta}{\partial \zeta^2}$, $\frac{\partial^2 \sigma}{\partial z^2} = \frac{1}{z_0^2} \frac{\partial^2 \sigma}{\partial \zeta^2}$ the equations

$$\begin{split} \frac{t_1}{t_0} \frac{\partial \eta(\tau,\zeta)}{\partial \tau} &= -\eta^3 + \frac{3}{2} \eta_0 \eta^2 - m \eta^2 + \frac{1}{2} \sigma \eta^2 - \frac{1}{2} \eta + m \eta - \frac{1}{2} \sigma \eta + \frac{z_1^2}{z_0^2} \frac{\partial^2 \eta(\tau,\zeta)}{\partial \zeta^2}, \\ \frac{t_1}{t_0} \frac{\partial \sigma(\tau,\zeta)}{\partial \tau} &= \frac{1}{6} \eta^3 - \frac{1}{4} \eta^2 - \beta \sigma, \end{split}$$

and choose again

$$\frac{t_1}{t_0} = \tau_0,$$

$$\frac{z_1^2}{z_0^2} = \varepsilon^2.$$

Accordingly is

$$\begin{split} \tau_0 \frac{\partial \eta(\tau,\zeta)}{\partial \tau} &= -\eta^3 + \left(\frac{3}{2} - \left(m - \frac{1}{2}\sigma\right)\right)\eta^2 \\ &- \left(\frac{1}{2} - \left(m - \frac{1}{2}\widetilde{\sigma}\right)\right)\eta + \varepsilon^2 \frac{\partial^2 \eta(\tau,\zeta)}{\partial \zeta^2} \\ &= \eta(1 - \widetilde{\eta})\left(\eta - \frac{1}{2} + m - \frac{1}{2}\sigma\right) + \varepsilon^2 \frac{\partial^2 \eta(\tau,\zeta)}{\partial \zeta^2}, \end{split} \tag{A.13}$$

$$\tau_0 \frac{\partial \sigma(\tau, \zeta)}{\partial \tau} = \frac{1}{6} \eta^3 - \frac{1}{4} \eta^2 - \beta \sigma. \tag{A.14}$$

The conserved equation for salinity is given by

$$t_1 \frac{\partial \sigma(t, z)}{\partial t} = -z_1^2 \frac{\partial^2}{\partial z^2} \left(\frac{1}{6} \eta^3 - \frac{1}{4} \eta^2 - \beta \sigma \right), \tag{A.15}$$

$$\frac{t_1}{t_0} \frac{\partial \sigma(\tau, \zeta)}{\partial \tau} = -\frac{z_1^2}{z_0^2} \frac{\partial^2}{\partial \zeta^2} \left(\frac{1}{6} \eta^3 - \frac{1}{4} \eta^2 - \beta \frac{z_1^2}{z_0^2} \sigma \right), \tag{A.16}$$

$$\tau_0 \frac{\partial \sigma(\tau, \zeta)}{\partial \tau} = -\varepsilon^2 \frac{\partial^2}{\partial \zeta^2} \left(\frac{1}{6} \eta^3 - \frac{1}{4} \eta^2 - \beta \sigma \right), \tag{A.17}$$

and the corresponding dimensionless Landau–Ginzburg free energy density φ_{LG} of Eq. (A.2)

$$\varphi_{LG} = \underbrace{\frac{1}{4}\eta^4 - \left(\frac{1}{2} - \frac{1}{3}\left(m - \frac{1}{2}\sigma\right)\right)\eta^3 + \left(\frac{1}{4} - \frac{1}{2}\left(m - \frac{1}{2}\sigma\right)\right)\eta^2 + \frac{\beta}{2}\sigma^2}_{\varphi_L} + \underbrace{\frac{1}{2}\varepsilon^2\left(\frac{\partial\eta}{\partial\zeta}\right)^2}_{}.$$
(A.18)

A.5. Irreversibility

A large number of Euler–Lagrange functions can be found which are invariant with respect to time reversal, that means, either there is only reversible processes or equations which do not contain "time" as an explicit parameter. It requires to introduce a non-equilibrium entropy, a Boltzmann H-theorem, a projection operator or similar assumptions [49,68–72] to achieve symmetry breaking in time. The time-dependent term $\tau_0 \frac{\partial \eta}{\partial x}$ in

$$\tau_0 \frac{\partial \eta(\tau, \zeta)}{\partial \tau} = \eta \left(\eta - 1 \right) \left(-\eta + \frac{1}{2} - m \right) + \varepsilon^2 \frac{\partial^2 \eta(\tau, \zeta)}{\partial r^2} \tag{A.19}$$

is based on this additional assumption and not a result of the variation and was only postulated. This expression can be interpreted as a deterministic equivalent to a random assumption. Only for the special case of a running wave it is possible to specify a Lagrange function for the equation of motion, that includes the time τ .

Data availability

No data was used for the research described in the article.

References

- B. Guillot, A reappraisal of what we have learnt during three decades on computer simulation of water, J. Mol. Liq. 101 (2002) 219–260.
- [2] L. Vrbka, P. Jungwirth, Brine rejection from freezing salt solutions: A molecular dynamics study, Phys. Rev. Lett. 95 (2005) 148501–1–14850–4.
- [3] F.J. Millero, R. Feistel, D.G. Wright, T.J. McDougall, The composition of standard seawater and the definition of the reference-composition salinity scale, Deep-Sea Res. I 55 (2008) 50–72.
- [4] D.N. Thomas, G.S. Dieckmann, Sea Ice, second ed., Wiley-Blackwell, Oxford, 2010.
- [5] B.C. Christner, C.E. Morris, C.M. Foreman, R. Cai, D.C. Sands, Ubiquity of biological ice nucleators in snowfall, Science 319 (2008) 1214.
- [6] R. Pandey, K. Usui, R.A. Livingstone, S.A. Fischer, J. Pfaendtner, E.H.G. Backus, Y. Nagata, J. Fröhlich-Nowoisky, L. Schmüser, S. Mauri, J.F. Scheel, D.A. Knopf, U. Pöschl, M. Bonn, T. Weidner, Ice-nucleating bacteria control the order and dynamics of interfacial water, Sci. Adv. (2016) e1501630, http://dx.doi.org/10. 1126/sciadv.1501630.
- [7] U. Nakaya, Snow Crystals, Harvard University Press, Cambridge, 1954.
- [8] J. Gravner, D. Griffeath, Modeling snow crystal growth II: A mesoscopic lattice map with plausible dynamics, Phys. D 237 (2008) 385–404, http://dx.doi.org/ 10.1016/j.physd.2007.09.008.
- [9] J. Gravner, D. Griffeath, Modeling snow crystal-growth: A three-dimensional mesoscopic approach, Phys. Rev. E 79 (2009) 011601, http://dx.doi.org/10. 1103/PhysRevE.79.011601.
- [10] K.G. Libbrecht, Explaining the formation of thin ice crystal plates with structure-dependent attachment kinetics, J. Cryst. Growth 253 (2003) 168–175.

- [11] K.G. Libbrecht, The physics of snow crystals, Rep. Progr. Phys. 68 (2005) 855–895, http://dx.doi.org/10.1088/0034-4885/68/4/R03.
- [12] D.A. Kessler, J. Koplik, H. Levine, Pattern selection in fingered growth phenomena, Adv. Phys. 37 (1988) 255–339.
- [13] D. Bensimon, Stability of viscous fingering, Phys. Rev. A 33 (1986) 1302–1309.
- [14] D. Bensimon, L.P. Kadanoff, S. Liang, B.I. Shraiman, C. Tang, Viscous flows in two dimensions, Rev. Mod. Phys. 58 (1986) 977–1002.
- [15] A.A. Wheeler, in: D.T.J. Hurle (Ed.), Description of Transport Processes in Handbook of Crystal Growth, in: Handbook of Crystal Growth, vol. 1b, North Holland, Amsterdam, London, New York, Tokyo, 1993.
- [16] G. Caginalp, J.T. Lin, A numerical analysis of an anisotropic phase field model, J. Appl. Math. 39 (1987) 51–66.
- [17] G. Caginalp, P.C. Fife, Dynamics of layered interfaces arising from phase boundaries, J. Appl. Math. 48 (1988) 506–518.
- [18] G. Caginalp, Stefan and Hele-Shaw type models as asymptotic limits of the phase-field equations, Phys. Rev. A 39 (1989) 5887–5896.
- [19] G. Caginalp, The dynamics of a conserved phase field system: Stefan-like, Hele-Shaw, and Cahn-Hilliard models as asymptotic limits, J. Appl. Math. 44 (1990) 77–94
- [20] G. Caginalp, Phase field models and sharp interface limits: Some differences in subtle situations, Rocky Mountain J. Math. 21 (1991) 603–616.
- [21] I.C. Kim, Homogenization of the free boundary velocity, Arch. Ration. Mech. Anal. 185 (2007) 69–103, http://dx.doi.org/10.1007/s00205-006-0035-3.
- [22] R.F. Sekerka, Morphology: from sharp interface to phase field models, J. Cryst. Growth 264 (2004) 530–540.
- [23] R. Almgren, W.-S. Dai, V. Hakim, Scaling behavior in anisotropic hele-shaw flow, Phys. Rev. Lett. 71 (1993) 3461–3464.
- [24] E. Ben-Jacob, N. Goldenfeld, J.S. Langer, G. Schön, Dynamics of interfacial pattern formation, Phys. Rev. Lett. 51 (1983) 1930–1932.
- [25] E. Ben-Jacob, N. Goldenfeld, B.G. Kotliar, J.S. Langer, Pattern selection in dendritic solidification, Phys. Rev. Lett. 53 (1984) 2110–2113.
- [26] E. Ben-Jacob, N. Goldenfeld, J. Koplik, H. Levine, T. Mueller, L.M. Sander, Experimental demonstration of the role of anisotropy in interfacial pattern formation, Phys. Rev. Lett. 55 (1985) 1315–1320.
- [27] E. Ben-Jacob, R. Godbey, N.D. Goldenfeld, J.S. Langer, G. Schön, Boundary-layer model of pattern formation in solidification, Phys. Rev. A 29 (1984) 330–340.
- [28] D.A. Kessler, J. Koplik, H. Levine, Geometrical models of interface evolution. II. numerical simulation, Phys. Rev. A 30 (1984) 3161–3174.
- [29] D.A. Kessler, J. Koplik, H. Levine, Numerical simulation of two-dimensional snowflake growth, Phys. Rev. A 30 (1984) 2820–2823.
- [30] D.A. Kessler, J. Koplik, H. Levine, Steady-state dendritic crystal growth, Phys. Rev. A 33 (1986) 3352–3357.
- [31] R.C. Brower, D.A. Kessler, J. Koplik, H. Levine, Geometrical approach to moving-interface dynamics, Phys. Rev. Lett. 51 (1983) 1111–1114.
- [32] R.C. Brower, D.A. Kessler, J. Koplik, H. Levine, Geometrical models of interface evolution, Phys. Rev. A 29 (1984) 1135–1142.
- [33] O. Penrose, P.C. Fife, Thermodynamically consistent models of phase-field type for the kinetics of phase transitions, Phys. D 43 (1990) 44–62.
- [34] M. Brokate, J. Sprekels, Hysteresis and Phase Transitions, Springer-Verlag, New York, Berlin, Heidelberg, 1996.
- [35] R. Kobayashi, Modeling and numerical simulations of dendritic crystal growth, Phys. D 63 (1993) 410–423.
- [36] R. Kobayashi, A numerical approach to three-dimensional dendritic solidification, Exp. Math. 3 (1994) 59–81.
- [37] A.A. Wheeler, B.T. Murray, R.J. Schaefer, Computation of dendrites using a phase field model, Phys. D 66 (1993) 243–262.
- [38] L. Gránásy, Cahn Hilliard-type density functional calculations for homogeneous ice nucleation in undercooled water. J. Mol. Struct. 485 (1999) 523–536.
- [39] P.R. Harrowell, D.W. Oxtoby, On the interaction between order and a moving interface: Dynamical disordering and anisotropic growth rates, J. Chem. Phys.
- 86 (1987) 2932–2942, http://dx.doi.org/10.1063/1.452044.
 [40] D. Grandi, A phase field approach to solidification and solute separation in water solutions, Z. Angew. Math. Phys. 64 (2013) 1611–1624, http://dx.doi.org/10. 1007/s00033-013-0301-9.
- [41] L.D. Landau, V.L. Ginzburg, On the Theory of Supercoductivity, Collected Papers of L. D. Landau, Gordon and Breach, Science Publishers, New York, London, Paris, 1965, pp. 546–568.
- [42] K. Morawetz, S. Thoms, B. Kutschan, Formation of brine channels in sea ice, Eur. Phys. J. E 40 (2017) 25, http://dx.doi.org/10.1140/epie/i2017-11512-x.
- [43] A. Umantsev, Field Theoretic Method in Phase Transformation, Springer Nature Switzerland AG, 2023.
- [44] H. Kleinert, Path Integrals in Quantum Mechanics, Statistics, Polymer Physics, and Financial Markets, 5th Edition, World Scientific, New Jersey, 2009.
- [45] H. Haug, Statistische Physik, Friedr. Vieweg & Sohn Verlagsgesellschaft mbH, Braunschweig/Wiesbaden, 1997.
- [46] R. Rajaraman, Solitons and Instantons, North Holland Publishing Company, Amsterdam, New York, Oxford, 1982.
- [47] O.A. Karim, A.D.J. Haymet, The ice/water interface: A molecular dynamics simulation study, J. Chem. Phys. 89 (1988) 6889–6096.

- [48] W.L. Jorgensen, J. Chandrasekhar, J.D. Madura, R.W. Impey, M.L. Klein, Comparision of simple potential functions for simulating liquid water, J. Chem. Phys. 79 (1983) 926–935, http://dx.doi.org/10.1063/1.445869.
- [49] N.G. van Kampen, Stochastic Processes in Physics and Chemistry, Elsevier, Amsterdam, Boston, Heidelberg, London, New York, Oxford, Paris, San Diego, San Francisco, Singapore, Sydney, Tokyo, 2007.
- [50] P.M.S.M. Cox, Exponential time differencing for stiff systems, J. Comput. Phys. 176 (2002) 430–455, http://dx.doi.org/10.1006/jcph.2002.6995.
- [51] W. Weidlich, G. Haag, Concepts and Models of a Quantitative Sociology, Springer-Verlag, Berlin, Heidelberg, New York, 1983.
- [52] J.G. Dash, H. Fu, J.S. Wettlaufer, The premelting of ice and its environmental consequences, Rep. Progr. Phys. 58 (1995) 115–167.
- [53] V.F. Petrenko, R.W. Whitworth, Physics of Ice, Oxford University Press, Oxford, New York, 1999.
- [54] D. Beaglehole, D. Nason, Transition layer on the surface on ice, Surf. Sci. 96 (1980) 357–363.
- [55] D. Beaglehole, P. Wilson, Thickness ans anisotropy of the ice-water interface, J. Phys. Chem. 97 (1993) 11053–11055.
- [56] H. Dosch, A. Lied, J.H. Bilgram, Glancing-angle x-ray scattering studies of the premelting of ice surfaces, Surf. Sci. 327 (1995) 145–164.
- [57] H. Dosch, A. Lied, J.H. Bilgram, Disruption of the hydrogen-bonding network at the surface of I_h ice near surface premelting, Surf. Sci. 366 (1996) 43–50.
- [58] Y. Furukawa, H. Nada, Anisotropic surface melting of an ice crystal and its relationship to growth forms, J. Phys. Chem. B 101 (1997) 6167–6170.
- [59] N.J. Robinson, B.S. Grant, C.L. Stevens, C.L. Stewart, M.J.M. Williams, Oceanographic observations in supercooled water: Protocols for mitigation of measurement errors in profiling and moored sampling, Cold Reg. Sci. & Technol. 170 (2020) 102954.
- [60] P.V. Hobbs, Ice Physics, Oxford University Press, Oxford, New York, Auckland Cape Town, Dar es Salaam, Hong Kong, Karachi, Kuala Lumpur, Madrid, Melbourne, Mexico City, Nairobi, New Dehli, Shanghai, Taipei, Toronto, 1974.
- [61] K.A. Jackson, D.R. Uhlmann, J.D. Hunt, On the nature of crystal growth from the melt, J. Chrystal Growth 1 (1967) 1–36.

- [62] A. Mori, M. Maruyama, Y. Furukawa, Second-order expansion of Gibbs-Thomson equation and melting point depression of ice crystallite, J. Phys. Soc. Japan 65 (1996) 2742–2744.
- [63] H. Nada, J.P. van der Eerden, An intermolecular potential model for the simulation of ice and water near the melting point: A six-site model of H₂O, J. Phys. Chem. B 188 (2003) 7401–7413.
- [64] G.T. Gao, X.C. Zeng, H. Tanaka, The melting temperature of proton-disordered hexagonal ice: A computer simulation of 4-site transferable intermolecular potential model of water, J. Chem. Phys. 112 (2000) 8534–8538.
- [65] M.J. Vlot, J. Huinink, J.P. van der Eerden, Free energy calculations on systems of rigid molecules: An application to the TIP4P model of H₂O, J. Chem. Phys. 110 (1999) 55–61.
- [66] B. Kutschan, K. Morawetz, S. Gemming, Modeling the morphogenesis of brine channels in sea ice, Phys. Rev. E 81 (2010) 036106, http://dx.doi.org/10.1103/ PhysRevE.81.036106.
- [67] S. Maus, The plate spacing of sea ice, Ann. Glaciol. 61 (2020) 408–425, http://dx.doi.org/10.1017/aog.2020.65.
- [68] E. Fick, G. Sauermann, Quantenstatistik Dynamischer Prozesse, Band 1, Akademische Verlagsgesellschaft Geest & Portig K.G. Leipzig, 1983.
- [69] E. Fick, G. Sauermann, Quantum Statistics of Dynamic Processes, Springer-Verlag, Berlin, Heidelberg, New York, London, Paris, Tokyo, Hong Kong, Barcelona, 1990.
- [70] H. Grabert, Projection Operator Techniques in Nonequilibrium Statistical Mechanics, Springer-Verlag, Berlin, Heidelberg, New York, 1982.
- [71] R. Zwanzig, Ensemble method in the theory of irreversibility, J. Chem. Phys. 33 (1960) 1338–1341, http://dx.doi.org/10.1063/1.1731409.
- [72] R. Zwanzig, On the identity of three generalized master equations, Physica 30 (1964) 1109–1123.

Further reading

 K.R. Subbaswamy, S.E. Trullinger, Instability of nontopological solitons of coupled scalar field theories in two dimensions, Phys. Rev. D 22 (6) (1980) 1495–1496